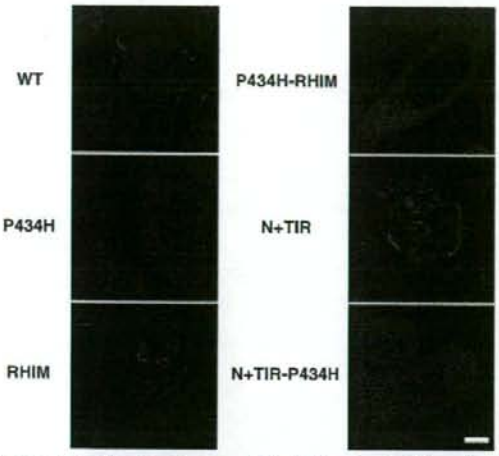

FIGURE 4. **Subcellular localization of TICAM-1 mutants.** HeLa cells were transfected with the indicated plasmids for FLAG-tagged wild-type TICAM-1 and TICAM-1 mutants and stained with anti-FLAG mAb followed by Alexa568-labeled goat anti-mouse Ab (*red*). Mutation of Pro^{434} in the TIR domain or mutation of the C-terminal RHIM domain affects the subcellular localization of TICAM-1. Nuclei were stained with DAPI (*blue*). *Bar*, 10 μm.

TICAM-1-mediated IRF-3 and NF-κB Activation Is Reduced by Mutations in the TIR or RHIM Domain—Based on the results of the yeast-two hybrid assay, we constructed several TICAM-1 mutants and examined their activities in mammalian cells (Fig. 3*A*). Only the TICAM-1 N+(TIR-P434H) mutant failed to activate both the IFN-β promoter and NF-κB, even after transfection of high concentrations of plasmid (Fig. 3*B*). The other mutants retained their IFN-β promoter and NF-κB activating abilities. However, transfection of the same concentration of plasmid resulted in increased protein expression of all TICAM-1 mutants compared with wild-type TICAM-1 protein expression (Fig. 3*C*). Subsequent normalization of the protein expression levels revealed that the signaling activities of these mutants were very weak compared with wild-type TICAM-1.

To examine the relationship between the reduced NF-κB and IFN-β promoter activation of each mutant and their homodimerizing activity, immunoprecipitation studies using HA- and FLAG-tagged constructs were performed. The homodimerizing activity was completely diminished in the dysfunctional N+(TIR-P434H) mutant (Fig. 3*D*). As observed in the yeast system, either the TIR domain or the C-terminal region enabled the TICAM-1 mutants to homodimerize in HEK293 cells. However, lack of either domain reduced the signaling activities of these mutants. These results suggest that full activation of TICAM-1 requires homodimerization at both the TIR domain and the C-terminal region.

Mutations of TICAM-1 Affect Its Subcellular Localization—To clarify the functional differences between wild-type TICAM-1 and the TICAM-1 mutants, we examined the subcellular localization of each FLAG-tagged mutant by confocal microscopy. As reported previously, we found that overexpression of wild-type TICAM-1 in HeLa cells leads to spontaneous activation of TICAM-1 and formation of speckle-like signalosomes (25) (Fig. 4, *upper left panel*). In contrast, the TICAM-1 P434H mutant localized diffusely in the cytosol with slight speckle formation (Fig. 4, *middle left panel*). A fiber-like staining pattern was observed in cells overexpressing the RHIM and N+TIR mutants, which contain the intact TIR domain but not the RHIM domain (*lower left* and *middle right panels*). The double P434H-RHIM mutant also localized diffusely with slight fiber-like formation (*upper right panel*). Finally, overexpression of the dysfunctional N+(TIR-P434H) mutant resulted in a completely diffuse staining pattern (*lower right panel*). These results suggest that Pro^{434} in the TIR domain is a critical for accumulation of TICAM-1 and formation of the fiber-like structures, whereas the RHIM domain is involved in the speckle formation of TICAM-1.

Association of RIP1 and TRAF3 with TICAM-1—To examine the relationship between the reduced activity of the TICAM-1 mutants and changes in their subcellular localization, we analyzed the co-localization of the downstream signaling molecules, RIP1 and TRAF3, with the TICAM-1 mutants by confocal microscopy and immunoprecipitation studies. RIP1 directly associates with TICAM-1 via the RHIM domain leading to activation of NF-κB (14, 15). When HeLa cells were co-transfected with FLAG-tagged RIP1 together with each of the HA-tagged TICAM-1 mutants, we found that RIP1 co-localized with wild-type TICAM-1 and the P434H mutant but not with the RHIM mutant (Fig. 5*A*). The association of RIP1 with these TICAM-1 mutants was confirmed by immunoprecipitation (Fig. 5*B*). As expected, the TICAM-1 mutants containing the mutated RHIM domain (P434H-RHIM) or a deleted C-terminal region (N+TIR) did not interact with RIP1 (data not shown).

Next we analyzed the association of the TICAM-1 mutants with TRAF3, a downstream signaling molecule that is essential for TICAM-1-mediated IRF-3 activation (17, 18). In contrast to RIP1, all of the TICAM-1 mutants with the exception of the dysfunctional N+(TIR-P434H) mutant, co-localized strongly with TRAF3 irrespective of their various localization patterns (Fig. 5*C*). Similar association profiles were observed in the immunoprecipitation studies (Fig. 5*D*), indicating that the mutation of the TIR and RHIM domains barely affected the recruitment of TRAF3. Our data suggest that, once TICAM-1 is oligomerized either through the TIR domain or the C-terminal region, TRAF3 is recruited to the N-terminal region of TICAM-1. Thus, association of TICAM-1 with RIP1 and TRAF3 is necessary but not sufficient for TICAM-1-mediated signaling.

NAP1 and TBK1 Are Recruited to the TICAM-1 Speckle-like Signalosomes—NAP1 has been identified as an essential molecule for TLR3- and RIG-1/MDA-5-mediated IRF-3 activation (16, 23). Because NAP1 directly binds to TBK1, an IRF-3-activating kinase (28), it is possible that NAP1 functions downstream of TRAF3. We examined the localization profile of NAP1 and TBK1 in cells co-expressing the TICAM-1 mutants. Importantly, NAP1 co-localized partially with only wild-type TICAM-1 (Fig. 6*A*). None of the TICAM-1 mutants used in this study co-localized with NAP1 even if the mutants were able to recruit TRAF3 (Fig. 6*A*). In addition, TBK1 also co-localized only with wild-type TICAM-1 (Fig. 6*B*). These results suggest that oligomerization induced by the TIR domain and the

C-terminal region in conjunction with RIP1 binding is required for speckle formation and recruitment of the IRF-3 kinase complexes that lead to effective activation of IRF-3 and NF-κB.

DISCUSSION

TLR3-TICAM-1 signaling results in transcriptional activation of various genes, including the type I IFN and IFN-regulatory genes. In this study, we examined the molecular mecha-

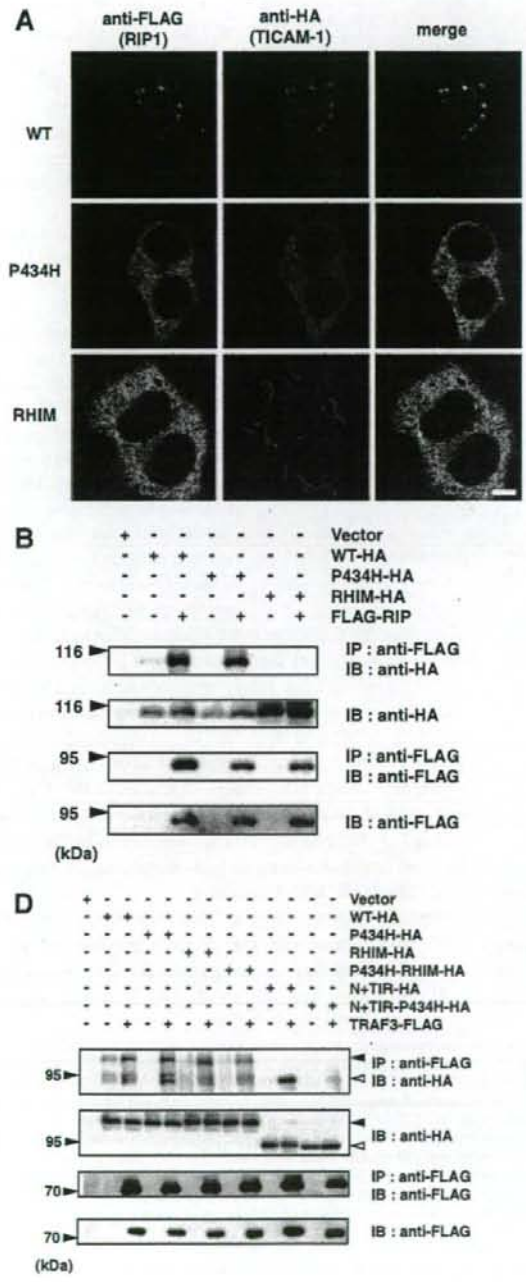

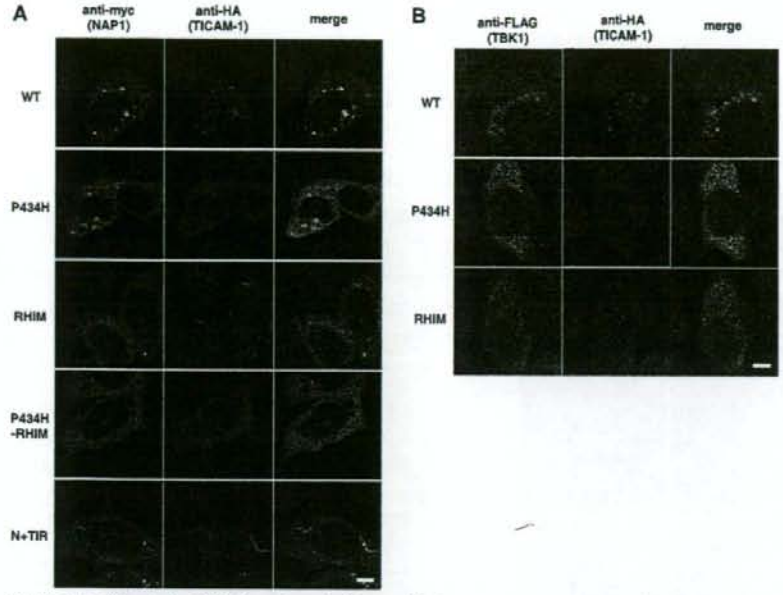

FIGURE 6. **Pro^{434} and the RHIM domain are indispensable for recruitment of NAP1 and TBK1 to TICAM-1.** Confocal images show HeLa cells co-expressing HA-tagged TICAM-1 mutants and Myc-tagged NAP1 (*A*) or FLAG-tagged TBK1 (*B*). *A*, HeLa cells, transfected with the indicated HA-tagged TICAM-1 mutants and Myc-tagged NAP1, were stained with anti-Myc mAb and anti-HA pAb, followed by Alexa488-labeled goat anti-rabbit Ab and Alexa568-labeled goat anti-mouse Ab. *B*, HeLa cells, transfected with the indicated HA-tagged TICAM-1 mutants and FLAG-tagged TBK1, were stained with anti-FLAG mAb and anti-HA pAb, followed by Alexa488-labeled goat anti-rabbit Ab and Alexa568-labeled goat anti-mouse Ab. *Green*, NAP1 (*A*) and TBK1 (*B*); *red*, wild-type and mutated TICAM-1; *blue*, DAPI-stained nuclei. *Bar*, 10 μm.

nism of TICAM-1-mediated signaling and demonstrated that TICAM-1 acts as a platform for recruitment of signaling molecules after homo-oligomerization at the TIR domain and C-terminal region. We show that Pro^{434} in the BB loop of the TIR domain is critical for TICAM-1 homo-oligomerization. Furthermore, the C-terminal region plays an important role in TICAM-1 signaling by inducing homo-dimerization and RIP1 recruitment to the RHIM domain. These results bring new insight into the molecular dynamics of TICAM-1 signaling and regulation of TLR3/4-mediated type I IFN production.

TLR signaling is mediated through TIR-containing adaptor molecules. The conserved proline residue in the BB loop of the TLR-TIR domain is crucial for binding the adaptor molecule (29). The TLR4 mutant P714H fails to bind TICAM-2 resulting in signaling off of TLR4-mediated signaling (9), whereas the dysfunctional TLR3 mutant A795H looses its TICAM-1-recruiting ability (7). Importantly, the TICAM-2-TIR mutant C117H bound the TLR4-TIR but failed to assemble homo (TICAM-2-TICAM-2)- and hetero (TICAM-2-TICAM-1)-dimers (9). Here, we show that Pro^{434} in the TIR domain of TICAM-1 is crucial for mediating interactions with TICAM-1-TIR but not with TLR3-TIR or TICAM-2-TIR. Thus, during TLR3/4-TICAM-1 signaling the BB loop of the upstream TIR determines the association with the downstream TIR domain.

TIR-containing adaptor molecules exhibit different molecular dynamics in response to stimulation by different TLRs. MyD88 is recruited to the plasma membrane or endosome and forms a signaling complex with receptors (30–32). Mal/TIRAP and TICAM-2/TRIF-related adaptor molecule, which associate with the plasma membrane via a phosphatidylinositol 4,5-bisphosphate-binding domain or myristoylation, respectively, act as a sorting adaptor to recruit MyD88 or TICAM-1 (33–35). During TLR4-mediated signaling, TICAM-1 may dissociate from the upstream adaptor TICAM-2 to form speckle-like signalosomes that induce type I IFN as observed during TLR3 signaling (25). Here, we show that TICAM-1 has two homo-dimerization motifs in the TIR domain and the C-terminal region. MyD88 also has the protein-protein interaction domain, the TIR and N-terminal death domain (36). Low molecular weight compounds that disrupt the TIR-TIR interaction of MyD88 have been synthesized to inhibit MyD88 signaling (37, 38). Homo-dimerization motifs of TICAM-1 would be good targets for designing chemical compounds that specifically block TICAM-1 signaling.

Several reports suggest that the C-terminal region of TICAM-1 is important for NF-κB activation and apoptosis in association with RIP1 binding to the RHIM domain but dispensable for IRF-3 activation (14, 15). In our study, decreased

FIGURE 5. **Association of RIP1 and TRAF3 with the TICAM-1 mutants.** *A*, confocal images of HeLa cells co-expressing FLAG-tagged RIP1 and HA-tagged TICAM-1 mutants. Cells were fixed and stained with anti-FLAG mAb and anti-HA pAb, followed by Alexa488-labeled goat anti-rabbit Ab and Alexa568-labeled goat anti-mouse Ab. RIP1 co-localizes with wild-type TICAM-1 and the P434H mutant. *Green*, RIP1; *red*, wild-type and mutated TICAM-1; *blue*, DAPI-stained nuclei. *Bar*, 10 μm. *B*, the RHIM domain of TICAM-1 is essential for association with RIP1. 293FT cells were transfected with the indicated HA-tagged TICAM-1 mutants and FLAG-tagged RIP1. After 24 h, cells were lysed and RIP1 was immunoprecipitated with anti-FLAG mAb. The immunoprecipitants were resolved on SDS-PAGE followed by immunoblotting with anti-HA pAb or anti-FLAG mAb. Total cell lysates were subjected to immunoblotting with anti-HA pAb or anti-FLAG mAb to detect protein expression (*IB*). *C*, confocal images of HeLa cells expressing FLAG-tagged TRAF3 and HA-tagged TICAM-1 mutants. HeLa cells were transfected with the indicated HA-tagged TICAM-1 mutants and FLAG-tagged TRAF3, and then stained with anti-FLAG mAb and anti-HA pAb, followed by Alexa488-labeled goat anti-rabbit Ab and Alexa568-labeled goat anti-mouse Ab. All TICAM-1 mutants except for N+TIR-P434H associate with TRAF3. *Green*, TRAF3; *red*, wild-type and mutated TICAM-1; *blue*, DAPI-stained nuclei. *Bar*, 10 μm. *D*, co-immunoprecipitation of TRAF3 with the TICAM-1 mutants. 293FT cells were transfected with the indicated HA-tagged TICAM-1 mutants and FLAG-tagged TRAF3. After 24 h, cells were lysed and TRAF3 was immunoprecipitated using an anti-FLAG mAb. Samples were resolved on SDS-PAGE followed by immunoblotting with anti-HA Ab or anti-FLAG mAb. Total cell lysates were subjected to immunoblotting with anti-HA pAb or anti-FLAG mAb to detect protein expression (*IB*).

NF-κB and IRF-3 activation was observed in cells overexpressing the TICAM-1 mutants with either a mutated RHIM motif or a deleted C-terminal region compared with cells overexpressing wild-type TICAM-1. These observations are consistent with a previous study using RIP1-deficient cells (39). In the presence of an apoptosis inhibitor, transfection of the same concentration of plasmid resulted in increased protein expression levels of these TICAM-1 mutants compared with wild-type TICAM-1. Why protein expression of the TICAM-1 mutants is higher than that of wild-type TICAM-1 remains question. However, it is possible that wild-type TICAM-1 is rapidly degraded via some protein modifications. RIP1 binding appears to be required for not only NF-κB activation but also IRF-3 activation. Indeed, our immunofluorescence data demonstrate that RIP1 has a critical role in the recruitment of NAP1 and TBK1 to the TICAM-1 speckle-like signalosomes. Because RIP1 associated with the TICAM-1 P434H mutant, it is possible that C-terminal region-mediated homodimerization may trigger RIP1 recruitment.

The TICAM-1 mutant (N+(TIR-P434H)) that lacks both homodimerization motifs failed to homodimerize resulting in abolishment its activity. However, mutants that lacked one homodimerization motif (P434H, P434H-RHIM, and N+TIR) were able to induce homodimerization. Remarkably, these mutants as well as the RHIM mutant recruited TRAF3 but not NAP1 or TBK1. TRAF3 has recently been identified as an essential molecule for TICAM-1-medated IRF-3 activation but not for NF-κB activation (17, 18). Direct interactions between TRAF3 and TICAM-1 were not observed in the yeast two-hybrid system (data not shown). Because TICAM-1 has a TRAF6 binding site at the N-terminal and TRAF2 also directly interacts with the N-terminal region of TICAM-1 (11, 40),[6] TRAF3 appears to form a molecular complex with TICAM-1 via TRAF2/6. In contrast to TRAF3, NAP1 and TBK1 co-localized partially with only wild-type TICAM-1. NAP1 has been identified as a TBK1-binding protein (28) that is involved in the recruitment of TBK1 to the N-terminal region of TICAM-1 (16). Because the TICAM-1 mutants, P434H and RHIM, did not co-localize with NAP1 and TBK1, oligomerization at two different sites in conjunction with RIP1 binding should be required for recruitment of the IRF-3 kinase complex. According to a proteolytic analysis, TICAM-1 possessed the protease-resistant structural domain at the N terminus. This domain was followed by the regions interacted with TRAF6, TRAF2, and TBK1. The TICAM-1 mutant that deleted the structural domain retained full IFN-inducing activity compared with wild-type TICAM-1.[7] One possible explanation why oligomerized TICAM-1 rather than monomer TICAM-1 can recruit downstream molecules is that in the monomer TICAM-1 the region associating with downstream signaling molecules is covered with the N-terminal structural domain. Once TICAM-1 is oligomerized at the TIR and C-terminal domains, the N-terminal region is exposed to interact with downstream molecules. The mechanism of how TICAM-1 recruits the IRF-3 kinase complex requires further investigation. Recent report suggests that TRAF3 ubiquitination facilitates the recruitment of TBK1 (41). We have also observed TICAM-1 phosphorylation and ubiquitination.[6] Structural analysis of the TICAM-1 molecule and characterization of protein modifications of signaling components are important for understanding the molecular topology for initiation of TICAM-1-mediated signaling.

[6] M. Sasai, H. Oshiumi, M. Matsumoto, and T. Seya, manuscript in preparation.
[7] M. Matsumoto, M. Sasai, and T. Seya, unpublished data.

Acknowledgments—We are grateful to M. Shingai, T. Ebihara, A. Ishii, and A. Matsuo for critical discussion. Thanks are also due to Dr. M. Nakanishi (Nagoya City University, Nagoya) and Dr. T. Taniguchi (Tokyo University, Tokyo) for providing plasmids.

REFERENCES

1. Akira, S., Uematsu, S., and Takeuchi, O. (2006) *Cell* **124,** 783–801
2. Yoneyama, M., Kikuchi, M., Natsukawa, T., Shinobu, N., Imaizumi, T., Miyagishi, M., Taira, K., Akira, S., and Fujita, T. (2004) *Nat. Immunol.* **5,** 730–737
3. Alexopoulou, L., Holt, A. C., Medzhitov, R., and Flavell, R. A. (2001) *Nature* **413,** 732–738
4. Matsumoto, M., Kikkawa, S., Kohase, M., Miyake, K., and Seya, T. (2002) *Biochem. Biophys. Res. Commun.* **293,** 1364–1369
5. Schulz, O., Diebold, S. S., Chen, M., Naslund, T. I., Nolte, M. A., Alexopoulou, L., Azuma, Y. T., Flavell, R. A., Liljestrom, P., and Reis e Sousa, C. (2005) *Nature* **433,** 887–892
6. Akazawa, T., Ebihara, T., Okuno, M., Okuda, Y., Shingai, M., Tsujimura, K., Takahashi, T., Ikawa, M., Okabe, M., Inoue, N., Okamoto-Tanaka, M., Ishizaki, H., Miyoshi, J., Matsumoto, M., and Seya, T. (2007) *Proc. Natl. Acad. Sci. U. S. A.* **104,** 252–257
7. Oshiumi, H., Matsumoto, M., Funami, K., Akazawa, T., and Seya, T. (2003) *Nat. Immunol.* **4,** 161–167
8. Yamamoto, M., Sato, S., Hemmi, H., Hoshino, K., Kaisho, T., Sanjo, H., Takeuchi, O., Sugiyama, M., Okabe, M., Takeda, K., and Akira, S. (2003) *Science* **301,** 640–643
9. Oshiumi, H., Sasai, M., Shida, K., Fujita, T., Matsumoto, M., and Seya, T. (2003) *J. Biol. Chem.* **278,** 49751–49762
10. Fitzgerald, K. A., Rowe, D. C., Barnes, B. J., Caffrey, D. R., Visintin, A., Latz, E., Monks, B., Pitha, P. M., and Golenbock, D. T. (2003) *J. Exp. Med.* **198,** 1043–1055
11. Sato, S., Sugiyama, M., Yamamoto, M., Watanabe, Y., Kawai, T., Takeda, K., and Akira, S. (2003) *J. Immunol.* **171,** 4304–4310
12. Sharma, S., tenOever, B. R., Grandvaux, N., Zhou, G. P., Lin, R., and Hiscott, J. (2003) *Science* **300,** 1148–1151
13. Fitzgerald, K. A., McWhirter, S. M., Faia, K. L., Rowe, D. C., Latz, E., Golenbock, D. T., Coyle, A. J., Liao, S. M., and Maniatis, T. (2003) *Nat. Immunol.* **4,** 491–496
14. Meylan, E., Burns, K., Hofmann, K., Blancheteau, V., Martinon, F., Kelliher, M., and Tschopp, J. (2004) *Nat. Immunol.* **5,** 503–507
15. Kaiser, W. J., and Offermann, M. K. (2005) *J. Immunol.* **174,** 4942–4952
16. Sasai, M., Oshiumi, H., Matsumoto, M., Inoue, N., Fujita, F., Nakanishi, M., and Seya, T. (2005) *J. Immunol.* **174,** 27–30
17. Hacker, H., Redecke, V., Blagoev, B., Kratchmarova, I., Hsu, L. C., Wang, G. G., Kamps, M. P., Raz, E., Wagner, H., Hacker, G., Mann, M., and Karin, M. (2006) *Nature* **439,** 204–207
18. Oganesyan, G., Saha, S. K., Guo, B., He, J. Q., Shahangian, A., Zarnegar, B., Perry, A., and Cheng, G. (2006) *Nature* **439,** 208–211
19. Kawai, T., Takahashi, K., Sato, S., Coban, C., Kumar, H., Kato, H., Ishii, K. J., Takeuchi, O., and Akira, S. (2005) *Nat. Immunol.* **6,** 981–988
20. Seth, R. B., Sun, L., Ea, C. K., and Chen, Z. J. (2005) *Cell* **122,** 669–682
21. Meylan, E., Curran, J., Hofmann, K., Moradpour, D., Binder, M., Bartenschlager, R., and Tschopp, J. (2005) *Nature* **437,** 1167–1172
22. Xu, L. G., Wang, Y. Y., Han, K. J., Li, L. Y., Zhai, Z., and Shu, H. B. (2005) *Mol. Cell* **19,** 727–740
23. Sasai, M., Shingai, M., Funami, K., Yoneyama, M., Fujita, T., Matsumoto, M., and Seya, T. (2006) *J. Immunol.* **177,** 8676–8683
24. Saha, S. K., Pietras, E. M., He, J. Q., Kang, J. R., Liu, S. Y., Oganesyan, G.,

Shahangian, A., Zarnegar, B., Shiba, T. L., Wang, Y., and Cheng, G. (2006) *EMBO J.* **25,** 3257–3263
25. Funami, K., Sasai, M., Ohba, Y., Oshiumi, H., Seya, T., and Matsumoto, M. (2007) *J. Immunol.* **179,** 6867–6872
26. Chen, C., and Okayama, H. (1987) *Mol. Cell. Biol.* **7,** 2745–2752
27. Tsujita, T., Tsukada, H., Nakao, M., Oshiumi, H., Matsumoto, M., and Seya, T. (2004) *J. Biol. Chem.* **279,** 48588–48597
28. Fujita, F., Taniguchi, Y., Kato, T., Narita, Y., Furuya, A., Ogawa, T., Sakurai, H., Joh, T., Itoh, M., Delhase, M., Karin, M., and Nakanishi, M. (2003) *Mol. Cell. Biol.* **23,** 7780–7793
29. Xu, Y., Tao, X., Shen, B., Horng, T., Medzhitov, R., Manley, J. L., and Tong, L. (2000) *Nature* **408,** 111–115
30. Latz, E., Visintin, A., Lien, E., Fitzgerald, K. A., Monks, B. G., Kurt-Jones, E. A., Golenbock, D. T., and Espevik, T. (2002) *J. Biol. Chem.* **277,** 47834–47843
31. Latz, E., Schoenemeyer, A., Visintin, A., Fitzgerald, K. A., Monks, B. G., Knetter, C. F., Lien, E., Nilsen, N. J., Espevik, T., and Golenbock, D. T. (2004) *Nat. Immunol.* **5,** 190–198
32. Honda, K., Yanai, H., Mizutani, T., Negishi, H., Shimada, N., Suzuki, N., Ohba, Y., Takaoka, A., Yeh, W. C., and Taniguchi, T. (2004) *Proc. Natl. Acad. Sci. U. S. A.* **101,** 15416–15421
33. Kagan, J. C., and Medzhitov, R. (2006) *Cell* **125,** 943–955
34. Rowe, D. C., McGettrick, A. F., Latz, E., Monks, B. G., Gay, N. J., Yamamoto, M., Akira, S., O'Neill, L. A., Fitzgerald, K. A., and Golenbock, D. T. (2006) *Proc. Natl. Acad. Sci. U. S. A.* **103,** 6299–6304
35. Fitzgerald, K. A., and Chen, Z. J. (2006) *Cell* **125,** 834–836
36. Burns, K., Martinon, F., Esslinger, C., Pahl, H., Schneider, P., Bodmer, J. L., Di Marco, F., French, L., and Tschopp, J. (1998) *J. Biol. Chem.* **273,** 12203–12209
37. Davis, C. N., Mann, E., Behrens, M. M., Gaidarova, S., Rebek, M., Rebek, J., Jr., and Bartfai, T. (2006) *Proc. Natl. Acad. Sci. U. S. A.* **103,** 2953–2958
38. Loiarro, M., Capolunghi, F., Fanto, N., Gallo, G., Campo, S., Arseni, B., Carsetti, R., Carminati, P., De Santis, R., Ruggiero, V., and Sette, C. (2007) *J. Leukoc. Biol.* **82,** 801–810
39. Cusson-Hermance, N., Khurana, S., Lee, T. H., Fitzgerald, K. A., and Kelliher, M. A. (2005) *J. Biol. Chem.* **280,** 36560–36566
40. Jiang, Z., Mak, T. W., Sen, G., and Li, X. (2004) *Proc. Natl. Acad. Sci. U. S. A.* **101,** 3533–3538
41. Kayagaki, N., Phung, Q., Chan, S., Chaudhari, R., Quan, C., O'Rourke, K. M., Eby, M., Pietras, E., Cheng, G., Bazan, J. F., Zhang, Z., Arnott, D., and Dixit, V. M. (2007) *Science* **318,** 1628–1632

Hepatol Int (2008) 2:222–230
DOI 10.1007/s12072-008-9055-4

ORIGINAL ARTICLE

Increased expression of Toll-like receptor 3 in intrahepatic biliary epithelial cells at sites of ductular reaction in diseased livers

Minoru Nakamura · Kenji Funami · Atsumasa Komori · Terufumi Yokoyama · Yoshihiro Aiba · Aiko Araki · Yasushi Takii · Masahiro Ito · Mutsumi Matsuyama · Makiko Koyabu · Kiyoshi Migita · Ken Taniguchi · Hikaru Fujioka · Hiroshi Yatsuhashi · Misako Matsumoto · Hiromi Ishibashi · Tsukasa Seya

Received: 23 August 2007 / Accepted: 23 January 2008 / Published online: 26 March 2008

Abstract *Background* Toll-like receptors (TLRs) may play active roles in both innate and adaptive immune responses in human intrahepatic biliary epithelial cells (HIBECs). The role of TLR3 expressed by HIBECs, however, remains unclear. *Methods* We determined the in vivo expression of TLRs in biopsy specimens derived from diseased livers immunohistochemically using a panel of monoclonal antibodies against human TLRs. We then examined the response of cultured HIBECs to a TLR3 ligand, polyinosinic–polycytidylic acid (polyI:C). Using siRNAs specific for Toll-IL-1R homology domain-containing adaptor molecule 1 (TICAM-1) and mitochondrial antiviral signaling protein (MAVS), we studied signaling pathways inducing IFN-β expression. *Results* The expression of TLR3 was markedly increased in biliary epithelial cells at sites of ductular reaction in diseased livers, including primary biliary cirrhosis (PBC), autoimmune hepatitis (AIH), and chronic viral hepatitis (CH) as compared to nondiseased livers. Although cultured HIBECs constitutively expressed TLR3 at both the protein and mRNA levels in vitro, the addition of polyI:C to culture media induced only minimal increases in IFN-β mRNA. In contrast, transfection of HIBECs with polyI:C induced a marked increase in mRNAs encoding a variety of chemokines/cytokines, including IFN-β, IL-6, and TNF-α. The induction of IFN-β mRNA was efficiently inhibited by an siRNA against MAVS but not against TICAM-1, indicating that the main signaling pathway for IFN-β induction following polyI:C transfection is via retinoic acid-inducible gene I (RIG-I)/melanoma differentiation-associated gene 5 (MDA5) in HIBECs. *Conclusions* TLR3 expression by biliary epithelial cells increased at sites of ductular reaction in diseased livers; further study will be necessary to characterize it's in vivo physiological role.

Keywords Primary biliary cirrhosis (PBC) · Human intrahepatic biliary epithelial cells (HIBECs) · Interferon beta (IFN-β) · Toll-like receptor 3 (TLR3) Toll-IL-1R homology domain-containing adaptor molecule 1 (TICAM-1) · Mitochondrial antiviral signaling protein (MAVS) · Retinoic acid inducible gene I (RIG-I) · Melanoma differentiation-associated gene 5 (MDA5)

Abbreviations

BEC	Biliary epithelial cell
CK	Cytokeratin
dsRNA	Double stranded RNA
ER	Endoplasmic reticulum
ELISA	Enzyme-linked immunosorbent assay
GAPDH	Glyceraldehydes-3-phosphate dehydrogenase
HIBEC	Human intrahepatic biliary epithelial cell
HRP	Horseradish peroxidase
IFN	Interferon

M. Nakamura (✉) · A. Komori · T. Yokoyama · Y. Aiba · A. Araki · Y. Takii · M. Ito · M. Matsuyama · M. Koyabu · K. Migita · K. Taniguchi · H. Fujioka · H. Yatsuhashi · H. Ishibashi
Clinical Research Center, National Hospital Organization (NHO) Nagasaki Medical Center, Kubara 2-1001-1, Omura, Nagasaki 856-8562, Japan
e-mail: nakamuram@nmc.hosp.go.jp

M. Nakamura
Department of Hepatology, Nagasaki University Graduate School of Biomedical Sciences, Kubara 2-1001-1, Omura, Nagasaki 856-8562, Japan

K. Funami · M. Matsumoto · T. Seya
Department of Microbiology and Immunology, Hokkaido University Graduate School of Medicine, Sapporo, Japan

IL	Interleukin
IRF	Interferon regulatory factor
MAVS	Mitochondrial anti-viral signaling protein
MDA5	Melanoma differentiation associated gene-5
MyD88	Myeloid differentiation factor 88
PBC	Primary biliary cirrhosis
PBMC	Peripheral blood mononuclear cells
PolyI:C	Polyinosinic–polycytidylic acid
PRR	Pattern-recognition receptor
RIG-I	Retinoic acid-inducible gene I
RT-PCR	Reverse transcription-polymerase chain reaction
siRNA	Small interfering RNA
TLR	Toll-like receptor
TNF	Tumor necrosis factor
TICAM-1	Toll-IL-1R homology domain containing adaptor molecule 1

Introduction

Epithelial cells are the first barrier against viral infection. Such cells typically express retinoic acid-inducible gene I (RIG-I)/melanoma differentiation-associated gene 5 (MDA5) and Toll-like receptor 3 (TLR3) to sense double-stranded RNAs (dsRNA), hallmarks of viral replication [1–3]. TLR3 is localized to endosomes and/or the cell surface in epithelial cells, while RIG-I/MDA5 resides in the cytoplasm [3–5]. TLR3-expressing epithelial cells are widely distributed throughout the body, with prominent expression in intestinal, cervical, uterine, endometrial, bronchial, and corneal epithelial cells, the central nervous system, and epidermal keratinocytes [6–16]. The function of TLR3 has been intensively studied in some of these epithelial cells; bronchial epithelial cells recognize dsRNA by cell-surface TLR3 and induce cellular responses, including the secretion of type 1 interferon (IFN) via the Toll-IL-1R homology domain-containing adaptor molecule 1 (TICAM-1)-interferon regulatory factor 3 (IRF3) signaling pathway [11, 12]. The intracellular RNA sensors RIG-I/MDA5 also serve as IFN inducers acting via the mitochondrial antiviral signaling protein (MAVS)-IRF3 signaling pathway, thus protecting host cells against the spread of viral invasion [2, 3].

We previously found that the expression of TLR3 and IFN-β mRNAs is significantly increased in both the portal areas and parenchyma of livers diseased with PBC [17]. There was a positive correlation between TLR3 and IFN-β mRNA levels in both areas, indicating that TLR3-type 1 IFN signaling pathway is activated in PBC; the TLR3-expressing and/or IFN-β-producing cells, however, remain unknown [17]. This prompted us to investigate TLR3 expression and IFN-β production in human intrahepatic biliary epithelial cells (HIBECs).

In this study, we used specific monoclonal antibodies against TLRs [4] to determine that intrahepatic bile ducts, but not hepatocytes, in diseased livers strongly express TLR3. TLR3 protein is found in HIBECs at low levels on the cell surface and high levels in endosomes. Our results, however, indicate that the primary signaling pathway for IFN-β induction activated by dsRNA functions via RIG-I/MDA5 in the cytoplasm but not via TLR3 expressed on the cell surface or in endosomes. This is contrary to results obtained for other types of epithelial cells, such as bronchial epithelial cells and endometrial cells, in which surface TLR3 recognizes viral dsRNA to signal the presence of infection via the TLR3-IRF3-type I interferon signaling pathway [9, 11, 12, 15]. Here we discuss dsRNA-sensing system functioning in HIBECs and the role of high expression levels of TLR3 in diseased livers.

Materials and methods

Liver biopsy specimen and immunohistochemical evaluation

Liver needle biopsy specimens, which were derived from seven primary biliary cirrhosis (PBC)-affected, five autoimmune hepatitis (AIH)-affected, and five chronic hepatitis C (CHC)-affected livers, were frozen in OCT compound (Sakura Finetechnical Co, Tokyo, Japan) immediately after the procedure and were stored at −80°C until use. Mouse monoclonal antibodies to human TLR1 (clone TLR1.136, IgG1, *k*), TLR2 (clone TLR2.45, IgG1, *k*), TLR3 (clone TLR3.7, IgG1, *k*), TLR4 (clone TLR4, IgG2a, *k*), and TLR6 (clone TLR6.127, IgG1, *k*) were generated in our laboratory [4]. Among these monoclonal antibodies, the specificity of anti-TLR3 (TLR3.7) was intensively studied. Anti-TLR3 monoclonal antibody specifically binds to the extracellular part of native TLR3 but not to denatured form of TLR3 or other TLRs, including TLR2 and TLR4. Furthermore, TLR3.7 inhibits dsRNA-induced IFN-β production by inhibiting the interassociation between dsRNA and TLR3 [4, 5]. Mouse monoclonal antibodies specific for cytokeratin (CK) 7 and CK 19 were purchased from DAKO (DAKO Japan, Kyoto, Japan). Frozen sections, 4 mm in thickness, were stained with anti-TLR and anti-CK7 or -CK19 antibodies as described elsewhere [17]. Briefly, frozen sections were first fixed in 50 and 100% acetone for 30 s and 3 min, respectively, followed by treatment with Peroxidase Blocking agent (DAKO) for 10 min. Sections were then incubated with anti-TLR monoclonal antibodies (anti-TLR1, 2, 3, 4, and 6) for 60 min at room temperature. A standard 2-step method with ENVISION+ (DAKO) was used to visualize bound antibody using 3,3′-diaminobenzidine as a chromogen

(DAKO); samples were also counterstained with Mayer's hematoxylin (DAKO). Three frozen liver biopsy specimens, which revealed normal histology, were similarly studied as nondiseased livers.

Isolation and culture of human intrahepatic biliary epithelial cells

Human intrahepatic biliary epithelial cells (HIBECs) were isolated from noncancerous liver tissues of three patients who had undergone hepatic resection for intrahepatic cholangiocarcinoma [18]. Briefly, liver specimens were digested with type IV collagenase (100 U/ml) (Sigma–Aldrich, St. Louis, MO). HIBECs were isolated immunomagnetically using Dynabeads conjugated with an epithelium-specific antibody, BerEp4 (Dynal Biotech, Norway). HIBECs were expanded in HIBEC culture medium (DMEM containing 5 μg/ml insulin, 10 ng/ml epidermal growth factor [EGF], 1.0 ng/ml hepatocyte growth factor [HGF], 4×10^{-8} M dexamethasone and 10% fetal bovine serum). All experiments were performed using HIBECs between 5 and 10 passages, which were performed using PBS containing 0.05% trypsin and 0.53 mM EDTA.

We obtained three different HIBECs (BEC3, BEC4, and BEC5) from the three different donors; each cultured HIBEC demonstrated spindle to polygonal epithelial cell morphology, with 100% positivity for CK7 and CK19 as determined by immunostaining with anti-CK7 and -CK19 monoclonal antibodies (DAKO).

Immunostaining and flow-cytometric analysis of HIBECs

HIBECs were cultured to semiconfluence in a tissue culture-treated 8-chamber glass slides (BD Biosciences, Bedford, MA) in HIBEC culture medium. Immunostaining of these cultured cells was then performed in a similar manner as that described for frozen sections of liver biopsies [17]. In brief, HIBECs were fixed with acetone, treated with peroxidase-blocking agent, and incubated with anti-TLR (anti-TLR1, -2, -3, -4, and -6) and anti-CK7 or anti-CK19 monoclonal antibodies followed by visualization of bound antibodies using a standard 2-step method with ENVISION+ (DAKO).

For flow-cytometric analysis, HIBECs were first suspended in PBS containing 0.1% sodium azide and 0.1% bovine serum albumin before incubating with 5 μg mAb (clone TLR3.7, IgG1, *k*) for 30 min at 4°C. Cells were washed and counterstained with FITC-conjugated goat antimouse IgG $F(ab')_2$ for 30 min at 4°C. We then determined fluorescence intensity and mean fluorescence shifts by flow cytometry (FACSCalibur; Becton-Dickinson).

Stimulation of HIBECs with polyI:C

Polyinosinic–polycytidylic acid (PolyI:C) was purchased from Sigma–Aldrich and reconstituted in endotoxin-free PBS. Transfection reagents, Lipofectamine 2000 and DOTAP, were purchased from Invitrogen (Carlsbad, CA) and Roche (Basel, Switzerland), respectively.

Twenty-four hours prior to the start of polyI:C stimulation, we changed the culture medium from HIBEC culture medium to basal medium (1:1 mixture of Ham's F12 and DMEM supplemented with 10% FBS without insulin, EGF, HGF, and dexamethasone). HIBECs were then incubated in the presence of polyI:C (40 μg/ml) or transfected with polyI:C using Lipofectamine 2000 or DOTAP according to the manufacturer's instructions. Optimal conditions for transfection by Lipofectamine 2000 and DOTAP were 0.8 μg/well and 1.0 μg/well polyI:C, respectively, in a 12-well plate (Becton Dickinson, Franklin Lakes, NJ) (data not shown).

RNA extraction and quantitation of mRNA

Total RNA was isolated from HIBECs using an RNeasy MiniKit (QIAGEN, Hilden, Germany) according to the manufacturer's instructions. Following RNase-free DNase I (QIAGEN) treatment, we synthesized first-strand complementary DNAs (cDNA) from 1.0 μg total RNA using a SuperScript First-Strand Synthesis System (Invitrogen). PCR amplification utilized FAST DNA SYBR Green I (Roche), which allows for automated quantification of amplified products in real-time using a Light-Cycler (Roche). We purchased primer sets specific for IFN-γ, IL-6, TNF-α, IL-8, and TLR3 from Roche. One microliter of each reverse-transcribed cDNA was used for real-time PCR analysis. Initial denaturation was performed at 95°C for 10 min followed by 40 amplification cycles of denaturation at 95°C for 10 s, annealing at 68°C for 10 s, and extension at 72°C for 16 s. We performed a standard melting curve analysis for every quantitation. Results were expressed as the ratio of cytokine/chemokine cDNA to GAPDH cDNA copy numbers in individual samples. Changes in mRNA levels were expressed as fold induction.

Enzyme-linked immunosorbent assay (ELISA)

HIBEC culture supernatants were assessed for cytokine/chemokine secretion using ELISA kits specific for IFN-β (PBL Biomedical Laboratories, Piscataway, NJ) and TNF-α, IL-6, and IL-8 (Beckman Coulter, Fullerton, CA), according to the manufacturers' instructions. Absorbance at either 405 or 450 nm was measured using a microplate reader (Multiskan JX, Thermo electron corporation, Vantaa, Finland).

Effect of siRNA on IFN-β mRNA induction by polyI:C

Oligonucleotides used for siRNA knockdown analysis were purchased from Proligo (St. Louis, MO) (GFP: sense, gcagcacgacuucuucaagtt, and antisense, cuugaagaagucgugc ugctt, MAVS: sense, ccaccuugaugccugugaaca, and antisense, uucacaggcaucaagguggua, TICAM-1: sense, gaccaga cgccacuccaactt, and antisense, guuggagugggcgucugguctt).

BEC3 cells (2.5×10^5 per well) were plated on 12-well plates using basal medium 24 h before siRNA transfection. On day 0, we transfected each siRNA oligonucleotide into BEC3 using Lipofectamine 2000. After 24 h (on day 1), the culture medium was replaced with fresh basal medium. Forty-eight hours after siRNA transfection (on day 2), cells were stimulated with polyI:C (final concentration 40 μg/ml in phosphate-buffered saline), Lipofectamine 2000 (0.8 μg/well in 12-well plates) or DOTAP (1.0 μg/well in 12-well plates). Six hours after polyI:C stimulation, we purified total RNA from BEC3 cells using an RNeasy Mini kit (Qiagen). RT-PCR was performed using M-MLV Reverse transcriptase (Promega, Madison, WA). Quantitative PCR analyses were carried out on an iCycler iQ Real-Time detection system (Bio-Rad, Hercules, CA) using Platinum SYBR Green qPCR SuperMix-UDG with ROX (Invitrogen) using the following primers; β-actin: forward, cctggcacccagcacaat, and reverse, gccgatccacacggagtact; IFN-β: forward, caacttgcttggattcctacaaag, and reverse, tattcaagcctcccattcaattg; MAVS: forward, ggtacccgagtctcgtttcct, and reverse, ttgtcttcagcaaacggcatt; TICAM-1: forward, agcgccttcgacattc taggt, and reverse, aggagaaccatggcatgca [19]. Quantitative PCR data was analyzed by the $2^{-\Delta\Delta CT}$ methods [20].

Ethics board

This study was approved by the Ethics Board of our institute. We obtained written informed consent from each subject for use of their biopsy and operation samples to advance knowledge on the cause of PBC.

Results

HIBECs strongly express TLR3 molecule in vitro

Previous analysis of the expression of TLRs mRNA in HIBECs by RT-PCR revealed that mRNAs encoding TLR1, -2, -3, -4, -5, -6, and -9, but not TLR7 and -8, are constitutively expressed in HIBECs [18]. The expression of TLR proteins, however, has not been examined. In this study, we studied the expression of TLR proteins in HIBECs using mouse monoclonal antibodies against TLR1, -2, -3, -4, and -6 [4]. TLR3 was strongly expressed on HIBECs (Fig. 1c) at an intensity comparable to that of CK19, a marker of biliary epithelial cells in the liver (Fig. 1f). In contrast, TLR1, -2, and -4 were weakly expressed on HIBECs (Fig. 1a, b, d). Flow-cytometric analysis revealed that while TLR3 was strongly expressed in the cytoplasm (Fig. 2a), it was only weakly expressed at the cell surface of HIBECs (Fig. 2b).

Biliary epithelial cells strongly express TLR3 at sites of ductular reaction in vivo

We examined the expression of TLRs in vivo using frozen sections of liver needle biopsy specimens using the monoclonal antibodies to TLR1, -2, -3, -4, and -6. Again, TLR3 was strongly expressed by intrahepatic biliary epithelial cells, especially at sites of ductular reaction in all diseased livers affected by PBC (Fig. 3b), AIH (Fig. 3c), and CHC (Fig. 3d). TLR3 was only weakly expressed on small bile ducts in normal livers (Fig. 3a). TLR3 was not expressed in hepatocytes of either diseased or normal livers. Minimal expression of TLR1, -2, -4, and -6 was observed in either diseased or normal livers (data not shown).

Induction of IFN-β by polyI:C stimulation in HIBECs

We examined the induction of IFN-β by HIBECs cultured for 24 h in basal medium containing 0–160 μg/ml of polyI:C, a ligand for TLR3. IFN-β secretion was consistently undetectable in culture supernatants, as determined by ELISA (data not shown). IFN-β mRNA copy numbers were calculated as 0.00024 ± 0.00017/GAPDH (mean value $\pm$ SD, $n = 3$) in the basal state, which increased by 2.7- to 5.5-fold (0.0012 ± 0.0010/GAPDH, $n = 3$) after 4–8 h of polyI:C stimulation (Fig. 4a). The increase in IFN-β mRNAs, however, was not statistically significant ($P = 0.195$). In contrast, IFN-β mRNA expression was markedly increased by polyI:C transfection using Lipofectamine 2000 (Fig. 4b). Maximal induction reached approximately 150-fold 4–8 h after transfection. Approximately 250 pg/ml IFN-β was secreted into culture medium over a 24-h period after polyI:C transfection. These results suggest that TLR3, even when expressed on the cell surface of HIBECs, does not recognize extracellular polyI:C; instead, TLR3 localized to endosomes and/or RIG-I/MDA5 in the cytoplasm sense polyI:C in HIBECs.

We also examined the induction of other chemokine/cytokine mRNAs. We observed the potent induction of mRNAs encoding for IL-6 (basal level 0.019–0.052/GAPDH) and TNF-α (basal level 0.00072–0.00081/GAPDH) to levels 50- and 120-fold greater than baseline, respectively (Fig. 5b, c). We detected 4- to 6-fold induction of mRNA for IFN-α (basal level 0.0059–0.0128/

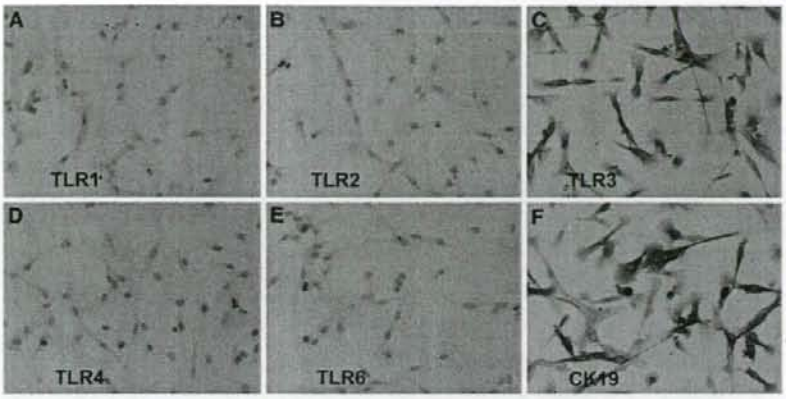

Fig. 1 TLRs immunostaining in cultured human intrahepatic biliary epithelial cells (HIBECs). BEC3 cells were stained with mouse monoclonal antibodies: (**a**) TLR1.136 (diluted 1/80); (**b**) TLR2.45 (diluted 1/100); (**c**) TLR3.7 (diluted 1/100); (**d**) HTA125 (diluted 1/70); (**e**) TLR6.127 (diluted 1/80); (**f**) anti-CK19 (diluted 1/200) for TLR1, TLR2, TLR3, TLR4, TLR6, and CK19, respectively, as described in the text. BEC3 cells stained strongly with TLR3.7 but only weakly with TLR1.136, TLR2.45, and HTA125

Fig. 2 Flow-cytometeric analysis of TLR3 in cultured human intrahepatic biliary epithelial cells (HIBECs). BEC3 cells were stained with TLR3.7 monoclonal antibody intracellularly (**a**) or extracellularly (**b**). BEC3 cells exhibited strong intracellular staining with TLR3.7 but only weak cell surface staining

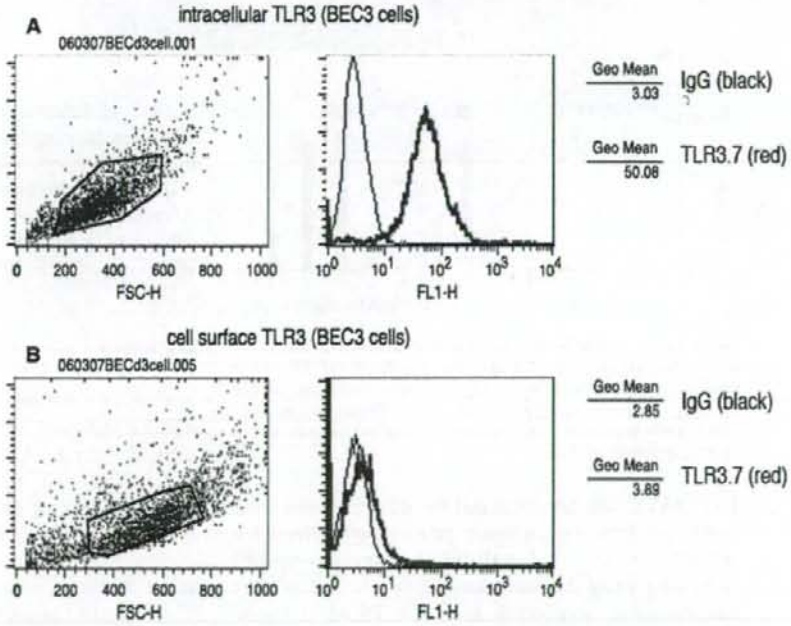

GAPDH), IL-8 (basal level 0.241–0.859/GAPDH), and TLR3 (basal level 0.0064–0.0081/GAPDH) (Fig. 5d–f). This upregulation in gene expression is also attributable to intracytoplasmic polyI:C recognition, since addition of polyI:C to culture medium did not induce any increase of mRNA levels for IL-6, TNF-α, IFN-α, IL-8, and TLR3 (data not shown).

Induction of IFN-β mRNA by polyI:C transfection depend on MAVS pathway but not on TICAM-1 pathway in HIBECs

To further confirm the functional role of TLR3 in the induction of IFN-β mRNA in HIBECs, we performed knockdown experiments using siRNA specific for TICAM-

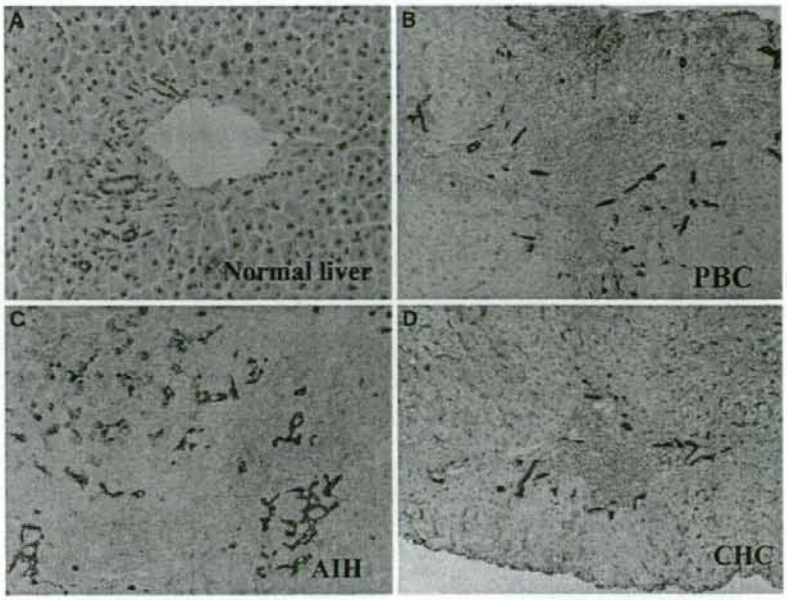

Fig. 3 In vivo expression of TLR3 in intrahepatic biliary epithelial cells. TLR3 was strongly expressed on intrahepatic biliary epithelial cells, especially at sites of ductular reactions, in livers from patients with PBC (**b**), AIH (**c**), and CHC (**d**). In contrast, TLR3 was weakly expressed on small bile ducts in normal liver (**a**)

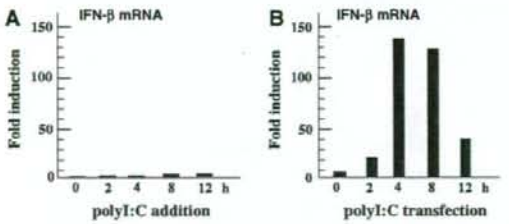

Fig. 4 Induction of IFN-β mRNA by polyI:C in HIBECs. BEC3 cells were either cultured in basal medium containing polyI:C (**a**) or transfected with polyI:C using Lipofectamine 2000 (**b**). mRNA encoding IFN-β was strongly induced by polyI:C-transfection, while IFN-β mRNA induction was minimal following the addition of polyI:C to culture medium

1 or MAVS. We first evaluated the efficiency of knockdown. Knockdown significantly reduced the mRNA levels of MAVS and TICAM-1 in HIBECs to approximately 30% of baseline using the corresponding siRNA (Fig. 6a). We then examined the effect of MAVS or TICAM-1 knockdown on the induction of IFN-β mRNA. As more efficient targeting of nucleotides to the endosomal compartment was reported by using DOTAP in comparison to Lipofectamine 2000 [21], we utilized DOTAP for the induction of IFN-β mRNA in knockdown experiments.

Interferon-β induction following polyI:C stimulation using Lipofectamine 2000 was largely dependent on MAVS/IPS-1, but not on TICAM-1 (Fig. 6b left side). Unexpectedly, similar results were obtained following polyI:C stimulation using DOTAP (Fig. 6b right side). These results suggested that the RIG-I/MDA5 (sensors of dsRNA in the cytosol)-MAVS signaling pathway plays a major role in the induction of IFN-β mRNA in HIBECs. Abundant expression of TLR3 in endosomes does not appear to participate significantly in polyI:C-mediated IFN-β induction in HIBECs.

Discussion

In this study, we provide the first data demonstrating that TLR3 is expressed in vitro in the cultured HIBECs; in these cells, IFN-β mRNA is strongly induced by polyI:C transfection, but only weakly induced by extrinsic polyI:C. Antibody blocking of TLR3 on HIBECs did not result in abrogation of IFN-β promoter activity, suggesting that cell-surface TLR3 participates only minimally in IFN-β promoter activation on dsRNA recognition (data not shown). These results suggested that endosomal, not cell surface, TLR3 is actively involved in type I IFN production by HIBECs. The results obtained by siRNA knockdown of TICAM-1 or MAVS, however, indicated that cytoplasmic RNA sensors like RIG-I/MDA5, not endosomal TLR3, are the major receptors initiating type I IFN induction in HIBECs.

To limit the growth of commensal organisms on their surface and to defend underlying tissues from invading pathogens, epithelial cells have both innate immune

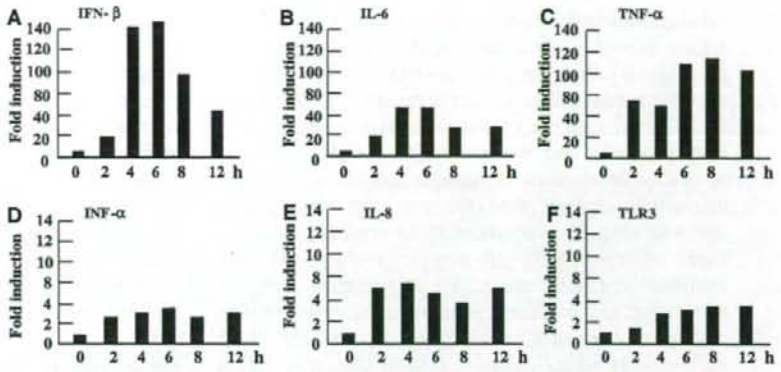

Fig. 5 Induction of chemokine/cytokine mRNAs in HIBECs following polyI:C-transfection. We observed strong induction of mRNAs encoding IFN-β (**a**), IL-6 (**b**), and TNF-α (**c**), but only weak induction of mRNAs for IFN-α (**d**), IL-8 (**e**), and TLR3 (**f**)

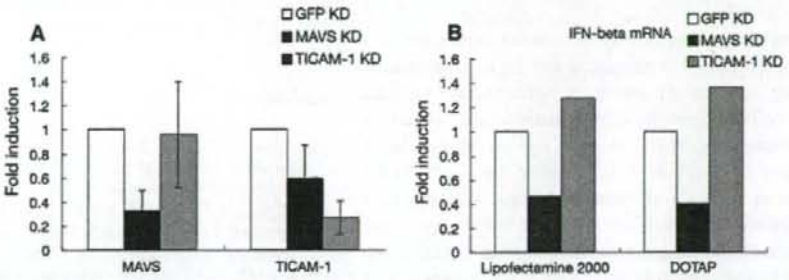

Fig. 6 Effect of MAVS or TICAM-1 knockdown on the induction of IFN-β mRNA following polyI:C transfection. mRNA levels of MAVS and TICAM-1 in HIBECs significantly decreased to 30% of baseline levels by knockdown using an appropriate siRNAs in HIBECs (**a**). The induction of IFN-β mRNA in HIBECs after polyI:C transfection was efficiently inhibited by MAVS but not by TICAM-1 knockdown (**b**)

antimicrobial functions and the ability to modulate the recruitment and activity of innate and adaptive immune system [1, 3]. Human fibroblasts, colon epithelial cells, lung epithelial cells, corneal epithelial cells and keratinocytes, as well as the respective cell lines, express TLR3 on their cell surfaces [4, 5, 7, 12, 14, 16]. Recent analyses of TLR3 subcellular localization, however, have suggested that TLR3 is localized to endoplasmic reticulum (ER) and early endosomes in most human epithelial cell types [5]. A similar localization of TLR3 was observed in HIBECs in the present study; the HIBECs express TLR3 on both the cell surface and within intracellular organelles.

Unexpectedly, surface TLR3 in HIBECs exerted only a weak ability to induce type I IFN in response to polyI:C. As polyI:C must be internalized and delivered to the ER or early endosomes, in which TLR3 is abundant, to activate TLR3, it was speculated that the capacity of HIBECs to internalize polyI:C is weak. Intracellular polyI:C that was internalized into cells by lipofection, however, did not play a major role in activating the type I IFN promoter via TLR3. These results indicate that even if the bile fluid contains dsRNA that may be derived from the gastrointestinal tract via the portal vein, hepatocytes or cholangiocytes infected with virus, or apoptotic cell debris, bile fluid only minimally stimulates TLR3 on the surface or in endosomes to induce type I IFN, although it is also possible that bile fluid may contain as yet unknown TLR3-ligand to induce type I IFN. Further studies of TLR3 in HIBECs will be needed to identify the functional specificities of the surface-expressed and endosome-expressed TLR3.

In this study, we also provide the first evidence that the expression of TLR3 by intrahepatic biliary epithelial cells is markedly increased at sites of ductular reaction in diseased livers, including those affected by PBC, AIH, and CHC. TLR3 protein expression increased in synovial tissues from patients with RA. In addition, cultured RA synovial fibroblasts were activated by the TLR3 ligand polyI:C and by RNA released from necrotic synovial fluid cells, suggesting that necrotic cells may act as an endogenous TLR3 ligand leading to the stimulation of proinflammatory gene expression and autoimmunity [22–24]. The overexpression of TLR3 in thyrocytes is associated with the development of Hashimoto's autoimmune thyroiditis [25]. TLR3 activation can drastically

enhance susceptibility to immune destruction of solid organs, as seen in autoimmune hepatitis [26]. Exposure of pancreatic β cells to the combination of dsRNA and IFN-α, -β, or -γ significantly increases apoptosis [27, 28]. TLR3 can directly trigger apoptosis in human umbilical vein endothelial cells and cancer cells [29, 30]. TLR3 plays a role in the development of hepatitis C-associated glomerulonephritis through the induction of mesangial cell apoptosis [31]. Thus, enhanced TLR3 expression in intrahepatic biliary epithelial cells may play a critical role in the induction and maintenance of inflammation, immune destruction, and/or biliary epithelial cell apoptosis in vivo in diseased liver such as PBC, whereas enhanced TLR3 expression in biliary epithelial cells in CHC may play a critical role for protecting them from hepatitis virus infection.

TLR3 in the nervous system induces the expression of a range of neuroprotective mediators and angiogenic factors, chemokines, and anti-inflammatory cytokines that regulate astrocyte cellular growth, differentiation, and migration [32]. Activation of TLR3 protects against DSS-induced acute colitis [33]. Thus, it is possible that high TLR3 expression in HIBECs at sites of ductular reaction may protect against cell death or stimulate tissue repair and regeneration by inducing the production of as yet unknown protective and/or growth factors. The strong expression of TLR3 at ductal plate in human fetal liver indicates the importance of TLR3 in the regeneration and/or development of biliary epithelial cells (data not shown). Therefore, it is also considered possible that as yet unknown TLR3-ligand is involved in the development of ductular reaction in diseased livers including PBC, AIH, and CHC.

Enhanced expression of various molecules, including MHC-class I and class II antigen, adhesion molecules (ICAM-1, VCAM-1, LFA-3, etc.), chemokines (MCP-1, SDF-1, Fractalkine, etc.), cytokines (IL-6, IL-8, TNF-α, etc.), costimulatory molecules (B7, PD-L1, PD-L2, etc.), and TLR4, have also been reported in biliary epithelial cells in livers affected by PBC [34–38]. In addition to these molecules involved in innate and acquired immune response, we here demonstrated for the first time that RIG-I/MDA5–MAVS signaling pathway is operative in the strong induction of IFN-β by dsRNA stimulation in HIBECs. TLR3 and RIG-I/MDA5 expression increase in the presence of IFN-α, IFN-β, IFN-γ, and TNF-α in vitro [39–43]. These results may indicate that intrahepatic biliary epithelial cells are involved as an immunoregulatory organ in various liver diseases, including PBC, AIH, and CHC. In addition, the portal inflammation is closely associated with ductular reaction in periportal areas. As hepatic stem cells are speculated to reside alongside biliary epithelial cells in canal of Hering [44, 45], the existence of multiple IFN-inducing pathways, including TLR3 and RIG-I/MDA5, may suggest the importance of this innate immune effector pathway in the protection of putative hepatic stem cells from viral infection.

In conclusion, we demonstrated for the first time the increased expression of TLR3 at sites of ductular reaction in diseased livers including PBC, AIH, and CHC. Since cytoplasmic RNA sensors like RIG-I/MDA5, not TLR3, seem to be the major receptors initiating strong type I IFN induction in biliary epithelial cells, we speculate that there is another important role in TLR3 that is highly expressed in biliary epithelial cells. Further study will be necessary to characterize its in vivo physiological role.

Acknowledgments This study was supported by Grants-in-Aid for Scientific Research from the Ministry of Health, Labour and Welfare of Japan and Grants-in-Aid for Scientific Research from the Japan Society for the Promotion of Science.

References

1. Akira S, Takeda K. Toll-like receptor signaling. Nat Rev Immunol 2004;4:499–511.
2. Yoneyama M, Kikuchi M, Natsukawa T, Shinobu N, Imaizumi T, Miyagoshi M, et al. The RNA helicase RIG-I has an essential function in double-stranded RNA-induced innate antiviral responses. Nat Immunol 2004;5:730–7.
3. Lee MS, Kim Y-J. Pattern-recognition receptor signaling initiated from extracellular, membrane, and cytoplasmic space. Mol Cells 2007;23:1–10.
4. Matsumoto M, Kikkawa S, Kohase M, Miyake K, Seya T. Establishment of a monoclonal antibody against human Toll-like receptor 3 that blocks double-stranded RNA-mediated signaling. Biochem Biophys Res Commun 2002;293:1364–9.
5. Matsumoto M, Funami K, Tanabe M, Hiroyuki O, Shingai M, Seto Y, et al. Subcellular localization of Toll-like receptor 3 in human dendritic cells. J Immunol 2003;171:3154–62.
6. Cario E, Podolsky DK. Differential alteration in intestinal epithelial cell expression of Toll-like receptor 3 (TLR3) and TLR4 in inflammatory bowel disease. Infect Immun 2000;68:7010–17.
7. Furrie E, Macfarlane S, Thomson G, Macfarlane GT. Toll-like receptors-2, -3 and -4 expression patterns on human colon and their regulation by mucosal-associated bacteria. Immunology 2005;115:565–74.
8. Schaefer TM, Desouza K, Fahey JV, Beagley KW, Wira CR. Toll-like receptor (TLR) expression and TLR-mediated cytokine/chemokine production by human uterine epithelial cells. Immunology 2004;112:428–36.
9. Jorgenson RL, Young SL, Lesmeister MJ, Lyddon TD, Misfeldt ML. Human endometrial epithelial cells cyclically express Toll-like receptor 3(TLR3) and exhibit TLR3-dependent responses to dsRNA. Human Immunol 2004;66:469–82.
10. Schaefer TM, Fahey JV, Wright JA, Wira CR. Innate immunity in the human female reproductive tract: antiviral response of uterine epithelial cells to the TLR3 agonist poly(I:C). J Immunol 2005;174:992–1002.
11. Guillot L, Goffic RL, Bloch S, Escriou N, Akira S, Chignard M, et al. Involvement of Toll-like receptor 3 in the immune response of lung epithelial cells to double-stranded RNA and influenza A virus. J Biol Chem 2005;280:5571–80.
12. Ritter M, Mennerich D, Weith A, Seither P. Characterization of Toll-like receptors in primary lung epithelial cells: strong impact

of the TLR3 ligand poly(I:C) on the regulation of Toll-like receptors, adaptor proteins and inflammatory response. J Inflamm 2005;2:16.
13. Kumar A, Zhang J, Yu FSX. Toll-like receptor 3 agonist poly(I:C)-induced antiviral response in human corneal epithelial cells. Immunology 2005;117:11–21.
14. Ueta M, Hamuro J, Kiyono H, Kinoshita S. Triggering of TLR3 by polyI:C in human corneal epithelial cells to induce inflammatory cytokines. Biochem Biophys Res Commun 2005;331:285–94.
15. Bsibsi M, Ravid R, Gveric D, van Noort JM. Broad expression of Toll-like receptors in the human central nervous system. J Neuropathol Exp Neurol 2002;61:1013–21.
16. Kollisch G, Kalali BN, Voelcker V, Wallich R, Behrendt H, Ring J, et al. Various members of the Toll-like receptor family contribute to the innate immune response of human epidermal keratinocytes. Immunology 2005;114:531–41.
17. Takii Y, Nakamura M, Ito M, Yokoyama T, Komori A, Shimizu-Yoshida Y, et al. Enhanced expression of type I interferon and Toll-like receptor-3 in primary biliary cirrhosis. Lab Invest 2005;85:908–20.
18. Yokoyama T, Komori A, Nakamura M, Takii Y, Kamihira T, Shimoda S, et al. Human intrahepatic biliary epithelial cells function in innate immunity by producing IL-6 and IL-8 via the TLR4-NF-γB and -MAPK signaling pathways. Liver Int 2006;26:467–76.
19. Sasai M, Shingai M, Funami K, Yoneyama M, Fujita T, Matsumoto M, et al. NAK-associated protein 1 participates in both the TLR3 and the cytoplasmic pathways in type I IFN induction. J Immunol 2006;177:8676–83.
20. Livak KJ, Schmittgen TD. Analysis of relative gene expression data using real-time quantitative PCR and the 2(-Delta Delta C (T)) method. Methods 2001;25:402.
21. Dalpke A, Frank J, Peter M, Heeg K. Activation of Toll-like receptor 9 by DNA from different bacterial species. Infect Immunol 2006;74:940–6.
22. Kariko K, Ni H, Capodici J, Lamphier M, Weissman D. mRNA is an endogenous ligand for Toll-like receptor 3. J Biol Chem 2004;279:12542–50.
23. Roelofs MF, Joosten LAB, Abdollahi-Roodsaz S, van Lieshout AWT, Sprong T, van den Hoogen FH, et al. The expression of Toll-like receptor 3 and 7 in rheumatoid arthritis synovium is increased and costimulation of Toll-like receptor 3, 4, and 7/8 results in synergistic cytokine production by dendritic cells. Arth Rheum 2005;52:2313–22.
24. Brentano F, Schorr O, Gay RE, Gay S, Kyburz D. RNA released from necrotic synovial fluid cells activates rheumatoid arthritis synovial fibroblasts via Toll-like receptor 3. Arth Rheum 2005;52:2656–65.
25. Harii N, Lewis CJ, Vasko V, McCall K, Benavides-Peralta U, Sun X, et al. Thyrocytes express a functional Toll-like receptor 3: overexpression can be induced by viral infection and reversed by phenylmethimazole and is associated with Hashimoto's autoimmune thyroiditis. Mol Endocrinol 2005;19:1231–50.
26. Lang KS, Georgiev P, Recher M, Navarini AA, Bergthaler A, Heikenwalder M, et al. Immunoprivileged status of the liver is controlled by Toll-like receptor 3 signaling. J Clin Invest 2006;116:2456–63.
27. Wen L, Peng J, Li Z, Wong FS. The effect of innate immunity on autoimmune diabetes and the expression of Toll-like receptors on pancreatic islets. J Immunol 2004;172:3173–80.
28. Rasschaert J, Ladriere L, Urbain M, Dogusan Z, Katabua B, Sato S, et al. Toll-like receptor 3 and STAT-1 contribute to double-stranded RNA+ interferon-γ-induced apoptosis in primary pancreatic β-cells. J Biol Chem 2005;280:33984–91.
29. Kaiser WJ, Kaufman JL, Offermann MK. IFN-γ sensitizes human umbilical vein endothelial cells to apoptosis induced by double-stranded RNA. J Immunol 2004;172:1699–710.
30. Salaun B, Coste I, Rissoan MC, Lebecque SJ, Renno T. TLR3 can directly trigger apoptosis in human cancer cells. J Immunol 2006;176:4894–901.
31. Wornle M, Schmid H, Banas B, Merkle M, Henger A, Roeder M, et al. Novel role of Toll-like receptor 3 in hepatitis C-associated glomerulonephritis. Am J Pathol 2006;168:370–86.
32. Bsibsi M, Persoon-Deen C, Verwer RWH, Meeuwsen S, Ravid R, Van Noort JM. Toll-like receptor 3 on adult human astrocytes triggers production of neuroprotective mediators. Glia 2006; 53:688–95.
33. Vijay-Kumar M, Wu H, Aitken J, Kolachala VL, Neish AS, Sitaraman SV, et al. Activation of Toll-like receptor 3 protects against DSS-induced acute colitis. Inflamm Bowel Dis 2007;13:856–64.
34. Harada K, Van de Water J, Leung PS, Coppel RL, Ansari A, Nakanuma Y, et al. In situ nucleic acid hybridization of cytokines in primary biliary cirrhosis: predominance of the TH1 subset. Hepatology 1997;25:791–6.
35. Harada K, Nakanuma Y. Molecular mechanisms of cholangiopathy in primary biliary cirrhosis. Med Mol Morphol 2006;39:55–61.
36. Gershwin ME, Nishio A, Ishibashi H, Lindor K. Primary biliary cirrhosis. In: Gershwin ME, Vierling JM, Manns MP, editors. Liver immunology, Chapter 20. Philadelphia, PA: Hanley & Belfus, Inc.; 2003. p. 311–27.
37. Kamihira T, Shimoda S, Nakamura M, Yokoyama T, Tkii Y, Kawano A, et al. Biliary epithelial cells regulate autoreactive T cells: implications for biliary-specific diseases. Hepatology 2005;41:151–9.
38. Wang AP, Migita K, Ito M, Takii Y, Daikoku M, Yokoyama T, et al. Hepatic expression of Toll-like receptor 4 in primary biliary cirrhosis. J Autoimmun 2005;25:85–91.
39. Heinz S, Haehnel V, Karaghiosoff M, Schwarzfischer L, Muller M, Krause SW, et al. Species-specific regulation of Toll-like receptor 3 genes in men and mice. J Biol Chem 2003;278:21502–9.
40. Tanabe M, Kurita-Taniguchi M, Takeuchi K, Takeda M, Ayata M, Ogura H, et al. Mechanism of up-regulation of human Toll-like receptor 3 secondary to infection of measles virus-attenuated strains. Biochem Biophys Res Commun 2003;311:39–48.
41. Tissari J, Siren J, Meri S, Julkunen I, Matikainen S. IFN-γ enhances TLR3-mediated antiviral cytokine expression in human endothelial and epithelial cells by up-regulating TLR3 expression. J Immunol 2005;174:4289–94.
42. Siren J, Imaizumi T, Sarkar D, Pietila T, Noah DL, Lin R, et al. Retinoic acid inducible gene-I and mda-5 are involved in influenza A virus-induced expression of anti-viral cytokines. Microbes Infect 2006;8:2013–20.
43. Liu P, Jamaluddin M, Li K, Garofalo RP, Casola A, Brasier AR. Retinoic acid-inducible gene I mediates early antiviral response and Toll-like receptor 3 expression in respiratory syncytial virus-infected airway epithelial cells. J Virol 2007;81:1401–11.
44. Theise ND, Saxena R, Portmann BC, Thung SN, Yee Y, Chiriboga L, et al. The canals of Hering and hepatic stem cells in humans. Hepatology 1999;30:1425–33.
45. Zhou H, Rogler LE, Teperman L, Morgan G, Rogler C. Identification of hepatocytic and bile ductular cell lineages and candidate stem cells in bipolar ductular reactions in cirrhotic human liver. Hepatology 2007;45:716–24.

Tumor-Secreted Lactic Acid Promotes IL-23/IL-17 Proinflammatory Pathway[1]

Hiroaki Shime,* Masahiko Yabu,* Takashi Akazawa,* Ken Kodama,† Misako Matsumoto,‡ Tsukasa Seya,‡ and Norimitsu Inoue[2]*

IL-23 is a proinflammatory cytokine consisting of a p19 subunit and a p40 subunit that is shared with IL-12. IL-23 is overexpressed in and around tumor tissues, where it induces local inflammation and promotes tumor development. Many tumor cells produce large amounts of lactic acid by altering their glucose metabolism. In this study, we show that lactic acid secreted by tumor cells enhances the transcription of *IL-23p19* and IL-23 production in monocytes/macrophages and in tumor-infiltrating immune cells that are stimulated with TLR2 and 4 ligands. DNA elements responsible for this enhancing activity of lactic acid were detected in a 2.7-kb 5′-flanking region of the human *IL-23p19* gene. The effect of lactic acid was strictly regulated by extracellular pH. Furthermore, by inducing IL-23 overproduction, lactic acid facilitated the Ag-dependent secretion of proinflammatory cytokine IL-17 but not IFN-γ by TLR ligand-stimulated mouse splenocytes. Interestingly, this effect was observed even in the absence of TLR ligand stimulation. These results suggest that rather than just being a terminal metabolite, lactic acid is a proinflammatory mediator that is secreted by tumor cells to activate the IL-23/IL-17 proinflammatory pathway but not the Th1 pathway. Targeting the lactic acid-induced proinflammatory response may be a useful approach for treating cancer. *The Journal of Immunology*, 2008, 180: 7175–7183.

Immune cells often infiltrate in and around many kinds of tumors. Initially, the immune system protects the host from cancer development and, indeed, the infiltration of NK cells in cancers is associated with a favorable prognosis (1). However, the infiltration of innate-immune cells such as macrophages correlates with a poor prognosis, which suggests that these cells may be directly involved in tumor development and metastasis by inducing angiogenesis and tissue remodeling. Moreover, many cancers often arise at sites of chronic inflammation caused by infections with microbes like *Helicobacter pylori* and hepatitis viruses. Noninfectious chronic inflammation such as that caused by asbestos is also associated with tumor development (1–3).

Infectious inflammation is associated with the secretion of several cytokines by innate immune cells in response to pathogen-associated molecular pattern stimuli (4). One of these cytokines is IL-23. IL-23 is a member of the proinflammatory heterodimeric cytokine family and consists of a p19 subunit and a p40 subunit that is shared with IL-12 (5, 6). Whereas IL-12 mainly induces the development of IFN-γ-producing Th1 cells, IL-23 is involved in maintaining the Th17 cells that are generated in response to IL-6 and TGF-β (7–10) and activates memory T cells ($CD44^{high}$ and $CD62L^{low}$) (11). IL-23 also induces the production of the proinflammatory cytokines IL-17 and IL-22 (11, 12). IL-23 is mainly produced by APCs, such as monocytes/macrophages and dendritic cells (DCs)[3] in response to stimulation with TLR2 and 4 ligands, such as peptidoglycan (PGN), LPS, and bacillus Calmette-Guérin cell wall skeleton (BCG-CWS) (13–15).

Recently, the Oft group (16) showed that IL-23 but not IL-12 is overexpressed by macrophages and DCs in human and mouse tumor tissues. They also showed that IL-23 is an important molecule that leads to the up-regulation of IL-17 and the matrix metalloprotease 9, to an increase in angiogenesis, and to a reduction in $CD8^+$ T cell infiltration in the tumor microenvironment (16). Significantly, IL-23p19-deficient mice but not IL-12p35-deficient mice developed chemically induced tumors less frequently than wild-type mice, and tumors transplanted into IL-23 receptor-deficient mice showed reduced growth (16). Furthermore, it was shown that Th17 cells are gradually increased in the tumor microenvironment during tumor development (17) and that IL-17 upregulates the production of a variety of proinflammatory cytokines (18) and proangiogenic factors (19) to promote tumor development (20). Therefore, the activation of the IL-23/IL-17 pathway promotes the incidence and growth of tumors by inducing local inflammatory responses. However, it remains unclear what induces inflammation and IL-23 overproduction in the tumor microenvironment. Notably, peripheral blood cells from patients with lung cancer that had been cultured with TLR stimuli overproduced IL-12/23p40; this response was eliminated in most patients after tumor resection (21). On the basis of these studies, we speculated that the tumor itself produces a factor(s) that promotes IL-23 overproduction. To test our hypothesis, we searched for tumor-secreted

*Department of Molecular Genetics and †Department of Surgery, Osaka Medical Center for Cancer and Cardiovascular Diseases, Osaka, Japan; and ‡Department of Microbiology and Immunology, Hokkaido University Graduate School of Medicine, Sapporo, Japan

Received for publication May 23, 2007. Accepted for publication March 23, 2008.

The costs of publication of this article were defrayed in part by the payment of page charges. This article must therefore be hereby marked *advertisement* in accordance with 18 U.S.C. Section 1734 solely to indicate this fact.

[1] This work was supported by a grant from the Cooperative Link of Unique Science and Technology for Economy Revitalization promoted by the Ministry of Education, Culture, Sports, Science and Technology of Japan and a Grant-in-Aid for Young Scientists from the Ministry of Education, Culture, Sports, Science, and Technology.

[2] Address correspondence and reprint requests to Dr. Norimitsu Inoue, Department of Molecular Genetics, Osaka Medical Center for Cancer and Cardiovascular Diseases, 1-3-3 Nakamichi, Higashinari-ku, Osaka 537-8511, Japan. E-mail address: inoue-no@mc.pref.osaka.jp

[3] Abbreviations used in this paper: DC, dendritic cell; PGN, peptidoglycan; BCG, bacillus Calmette-Guérin; CWS, cell wall skeleton; LDH, lactate dehydrogenase; MCT, monocarboxylate transporter; siRNA, small interfering RNA; Pam_3CSK_4, *N*-palmitoyl-*S*-[2,3-bis(palmitoyloxy)-(2*R*,*S*)propyl]-[*R*]-cysteinyl-[*S*]-seryl-[*S*]-lysl-[*S*]-lysl-[*S*]-lysl-[*S*]-lysine/HCl; BCECF, 2′,7′-bis-(2-carboxyethyl)-5-(and-6)-carboxyfluorescein/acetoxymethyl ester.

 0022-1767/08/$2.00

factors that might modulate the production of IL-23 by monocytes/macrophages stimulated with TLR ligands. In this study, we show that lactic acid secreted from tumor cells up-regulates TLR signal-dependent transcription of the IL-23p19 subunit in human and mouse monocytes/macrophages to enhance IL-23 secretion. Therefore, we predict that the lactic acid that is secreted by many tumor cells is a proinflammatory mediator that promotes tumor development.

Materials and Methods

Cell culture

The CADO-LC10 cell line, which was established from a human lung adenocarcinoma (22), was cultured in high glucose DMEM (4.5 mg/ml glucose; Sigma-Aldrich). Human PBMC, human monocytes, mouse splenocytes, the mouse macrophage-like cell line J774.1 (RIKEN cell bank), and the mouse melanoma cell line B16 were cultured in RPMI 1640 (Sigma-Aldrich). All media were supplemented with 10% heat-inactivated FCS, 100 U/ml penicillin, and 100 μg/ml streptomycin. Cells were cultured at 37°C under a 5% CO_2 atmosphere.

Reagents and Abs

We purchased the TLR ligands: PGN of *Staphylococcus aureus* and LPS from Sigma-Aldrich and a synthetic tripalmitoylated lipopeptide, Pam_3CSK_4, from InvivoGen. BCG-CWS was prepared as described previously (23, 24). L-Lactic acid was purchased from Sigma-Aldrich and Wako Pure Chemical and sodium lactate was purchased from WAKO. We used anti-mouse IL-23p19 Ab (G23-8; eBioscience) to neutralize IL-23 activity and rat IgG1 Ab (eBRG1; eBioscience) as an isotype control; both Abs were used at a concentration of 10 μg/ml. We purchased recombinant GM-CSF from PeproTech and anti-GM-CSF receptor α-chain Ab (S-20) from Santa Cruz Biotechnology.

Conditioned medium analysis

Conditioned medium was prepared from CADO-LC10 cells that had been cultured for 3 days. The medium was passed through a 0.22-μm pore size filter (Millipore) and stored at −80°C. For some experiments, the conditioned medium was subjected to molecular size fractionation by using Microcon YM-10 centrifugal filter devices, which separates molecules at the nominal 10-kDa molecular mass cutoff (Millipore). The flow-through fraction (<10 kDa) was supplemented with 10% FCS and the retentate (>10 kDa) was diluted with serum-free culture medium to obtain the original volume. In other experiments, the conditioned medium was treated with 50 μg/ml proteinase K at 37°C for 1 h. To remove proteinase K, the medium was passed through a Microcon YM-10 and the flow-through fraction was used for further experimentation. The control media were subjected to the same treatments as the conditioned media.

To examine how glucose concentrations in the culture medium of CADO-LC10 affects the subsequent enhancing activity of the conditioned medium, we cultured confluent CADO-LC10 cells for 3 days in fresh glucose-free DMEM (Invitrogen) supplemented with 1 or 4.5 mg/ml glucose and 10% FCS. In separate experiments, we inhibited lactic acid production by culturing the CADO-LC10 cells in the presence or absence of 20 mM oxamic acid (Sigma-Aldrich) for 2 days. The pH of the conditioned media and the lactic acid-containing media neutralized with NaOH was measured with a pH meter (Beckman Coulter) at 37°C under a 5% CO_2 atmosphere. L-Lactic acid concentrations in the conditioned media were measured by using a Determiner LA Kit (Kyowamedics). In the enhancing activity analysis, the conditioned media of CADO-LC10 cells described above were added to cells with an equal volume of cell culture media (i.e., 50% of the medium consisted of conditioned medium).

Measurement of cytokines

Human PBMC were isolated from healthy volunteers by using Ficoll-Paque Plus (GE Healthcare Bio-Sciences). Human monocytes were purified from the PBMC by using the MACS system (Miltenyi Biotec) and monocyte isolation kit II (Miltenyi Biotec). To measure human IL-23 production, 1.5×10^5 monocytes were cultured in 96-well tissue culture plates in the presence or absence of lactic acid for 24 h and then treated with 10 μg/ml PGN for 24 h. The IL-23, IL-12/23p40, and IL-6 levels in the culture supernatants were measured by using human IL-23 (Bender MedSystems), human IL-12p40, and human IL-6 (BioSource International) ELISA kits, respectively. To measure mouse IL-23 production, 1.0×10^5 J744.1 cells were stimulated with lactic acid and 10 μg/ml PGN. The measurements of mouse IL-23 production were performed by using a mouse IL-23 ELISA kit (eBioscience).

Mouse splenocytes isolated from an OVA-specific, MHC class II-restricted αβ TCR-transgenic mouse, OT-II (25), were cultured at 5×10^5 cells/well in 96-well tissue culture plates with 0.2 μg/ml $OVA_{323-339}$ peptides (Biosynth International) in the presence or absence of TLR ligands and lactic acid. After 4 days of incubation, the cytokines in the culture supernatants were measured by using IL-17A (R&D Systems) and IFN-γ (BioSource International) ELISA kits. These experiments using animals were conducted according to our institutional guidelines.

Real-time RT-PCR

Total RNA was isolated from cells by using the SV96 Total RNA Isolation System (Promega) according to the manufacturer's instructions, after which it was treated with RNase-free DNase I. cDNA was synthesized at 42°C for 50 min by using oligo$(dT)_{12-18}$ primers and SuperScript III reverse transcriptase in the presence of RNase inhibitor (Invitrogen). Diluted cDNA samples were mixed with a pair of primers derived from human *IL-23p19* or *β-actin* cDNA sequences and PCR was performed by using SYBR Green PCR master mix (Applied Biosystems) and an Applied Biosystems 7500HT sequence detection system. The following PCR primers were designed: for human *IL-23p19*, forward primer, 5′-AGTGTGGAG ATGGCTGTGACC-3′ and reverse primer, 5′-GCTGGGACTGAGGCT TGGAATCTG-3′; for human *IL-12/23p40*, forward primer, 5′-ATGCCGT TCACAAGCTCAAGTATG-3′ and reverse primer, 5′-GAACGCAGAAT GTCAGGGAGAAGT-3′; and for human *β-actin*, forward primer, 5′-TCA CCCACACTGTGCCCATCTACGA-3′ and reverse primer, 5′-CAGCGG AACCGCTCATTGCCAATGG-3′. Copy numbers were calculated from the amount of cDNA cloned into the pGEM-T easy vector (Promega) and normalized to *β-actin*. PCR for mouse *IL-23p19* and *β-actin* was performed by using the TaqMan PCR Core reagent kit, TaqMan probes, and primer sets of the TaqMan Gene Expression assay system (for *IL-23p19*, Mm00518984_m1 and for *β-actin*, Mm00607939_s1; Applied Biosystems). The relative expression of *IL-23p19* was normalized to that of *β-actin* and calculated by using the ΔΔCt method (16, 26).

Luciferase assay

A luciferase reporter plasmid for monitoring *IL-23p19* transcription was constructed as follows. A 6.7-kb fragment of the human *IL-23p19* gene from the *Sac*I site (−6654 bp) to the ATG initiation site that contained the 5′-flanking region and 5′-untranslated region of the gene was amplified by PCR using the RP11-348M3 clone (Research Genetics) as the template. The fragment was then subcloned between the *Sac*I and *Nco*I sites of the pGL3 promoter vector (Promega) to generate the p19–5′ luc vector. We also constructed a reporter gene plasmid containing the 2.7-kb 5′-flanking region of the human *IL-23p19* gene as follows. The p19–5′ luc plasmid was digested with *Sac*I and *Xma*I, treated with T4 DNA polymerase (Takara Bio), and self-ligated. We then inserted the *Xho*I and *Bam*H I fragments of the PGK promoter-driven neomycin resistance gene from pGKEM7-neoW into the *Sal*I and *Bam*H I sites of the plasmid to generate the p19–5′ 2.7k luc neo vector. The luciferase reporter plasmid for monitoring NF-κB activity was constructed as follows. The following synthetic oligonucleotides were annealed: 5′-TCGAGAAATGGGGACTTTCCGC TGGGGACTTTCCGCAAACCGC-3′ and 5′-GGTTTGCGGAAAGTCC CCAGCGGAAAGTCCCCATTTC-3′ (the underlined sequences indicate canonical NF-κB binding sites). The annealed oligonucleotides were then subcloned together with a *Sac*II/*Nco*I fragment of the minimal promoter sequence of the pNF-κB-Luc vector (Stratagene) between *Xho*I and *Nco*I sites of the pGL3 promoter vector containing the PGK promoter-driven neomycin resistance gene to generate the pGL3–2κB luc neo vector. J774.1 cells were then transfected with the p19-5′ luc vector and pGKEM7-neoW, the p19-5′ 2.7k luc neo vector, or pGL3–2κB luc neo vector by using FuGENE 6 (Roche) according to the manufacturer's instructions. The transfected cells were selected with 200 μg/ml G418. The cells were seeded in 96-well tissue culture plates at 1×10^4 cells/well and incubated with stimulants for 24 h as described above. After incubation, the cells were lysed with GloLysis buffer (Promega) and the luciferase activity was measured by using the Bright-Glo luciferase assay system (Promega) and a Mithras LB940 multimode reader (Berthold Technologies).

Small interfering RNA (siRNA)

We purchased *SMART*pool siRNA reagents for the human *LDHA* gene from Dharmacon and the Allstars negative control siRNA rhodamine from Qiagen. CADO-LC10 cells were transfected with siRNA (73 nM) by using XtremeGENE siRNA Transfection Reagent (Roche) according to the manufacturer's instructions. This transfection procedure was repeated on the second day to increase the RNA interference efficiency. On the fourth day,

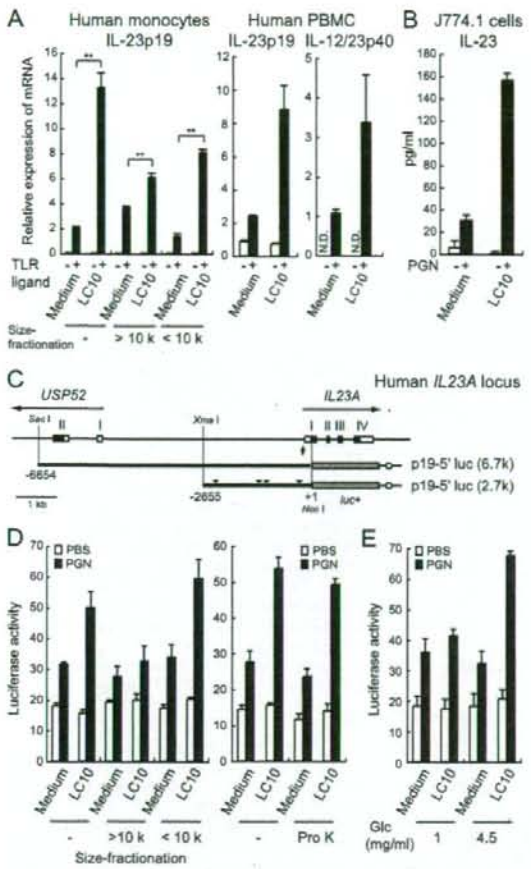

FIGURE 1. Tumor cell-conditioned medium enhances IL-23 expression in TLR ligand-stimulated monocytes/macrophages. *A*, Conditioned medium of the lung adenocarcinoma cell line CADO-LC10 enhances the TLR ligand-induced *IL-23p19* mRNA expression in human monocytes/macrophages (*left*). Human monocytes were stimulated with 10 μg/ml PGN (■) or PBS (□) in the presence (LC10) or absence (Medium) of 50% of the conditioned medium for 4 h. The conditioned medium was also fractionated according to molecular size, with the cutoff being at the nominal 10-kDa molecular mass (*left*). Human PBMC were stimulated with 5 μg/ml BCG-CWS in the presence or absence of the conditioned medium (*middle* and *right*). The relative expression of *IL-23p19* (*left* and *middle*) and *IL-12/23p40* (*right*) mRNA was measured by real-time RT-PCR and normalized to β-*actin* expression. N.D., Not detected. *B*, J774.1 cells were stimulated with 10 μg/ml PGN for 24 h in the presence or absence of the conditioned medium and the IL-23 that was secreted was measured by ELISA. *C*, Schematic representation of the human *IL23A* gene locus and two luciferase reporter genes carrying the 5′-flanking regions of the *IL-23p19* gene. The position from the translation start site (+1) is indicated in each construct. Shown are the untranslated regions (□), the coding region of *IL-23p19* and the *USP52* exon (■), the *luciferase* gene (▥), the SV40 late poly(A) signal (○), and the TATA box sequence (arrow). The arrowheads indicate putative NF-κB binding sites (−2311 to −2302, −1261 to −1252, −1049 to −1040, and −256 to −245) in the 2.7-kb 5′-flanking region. *D*, J774-p19-5′ luc cells were stimulated with 10 μg/ml PGN in the presence of the whole conditioned medium or the size-fractionated conditioned medium (*left*) or conditioned medium that had been treated with 50 μg/ml proteinase K (Pro K) for 1 h (*right*). Luciferase activity was then measured. *E*, Conditioned media were prepared from CADO-LC10 cells cultured in medium containing 1 or 4.5 mg/ml glucose (Glc). The control media (Medium) were subjected to the same treatments as the conditioned media (LC10). These media were added at 50% to determine the enhancing activity. The data represent mean values ± SD (n = 3). **, $p < 0.01$.

the cells were collected and plated at 1.4×10^6 cells/well in 12-well plates. After incubation for 24 h, we collected the conditioned medium and incubated the cells further for 24 h. The collected media were combined and used for further analysis. The expression of LDHA in siRNA-transfected CADO-LC10 cells was evaluated by performing semiquantitative RT-PCR and Western blotting. The following PCR primers were used: for human *LDHA*, forward primer, 5′-GCACGTCAGCAAGAGGGAGAAAG-3′ and reverse primer, 5′-AGGTAACGGAATCGGGCTGAATC-3′ and for human β-*actin*, forward primer, 5′-GCGGGAAATCGTGCGTGACATT-3′ and reverse primer, 5′-GATGGAGTTGAAGGTAGTTTCGTG-3′. Anti-LDHA (N-14; Santa Cruz Biotechnology) and anti-β-tubulin (TUB 2.1; Sigma-Aldrich) Abs were used for Western blotting. The expression levels of proteins were calculated by using Image J software (http://rsb.info.nih.gov/ij/) and were normalized to those of β-tubulin expression.

Measurement of intracellular pH

Intracellular pH was measured by using BCECF/AM (Invitrogen) (27). Fluorescence at 535 nm with excitation at 485 and 388 nm was measured for 0.1 s every 30 s after adding lactic acid or hydrochloric acid (WAKO) by using an ARVO MX 1420 multilabel counter (PerkinElmer).

Purification of tumor-infiltrating immune cells

Tumor-infiltrating immune cells were purified from tumors formed by B16 melanoma cells in C57BL/6 mice by using CD45 MACS MicroBeads (Miltenyi Biotec) as described previously (28). The purified cells were stained with FITC-conjugated anti-CD45.2 (104; eBioscience), FITC-conjugated anti-CD11b (M1/70; eBioscience), and PE-conjugated anti-CD11c (HL3; BD Biosciences) and examined by using the FACSCalibur system (BD Biosciences).

Statistical analyses

In measurement of cytokines, real-time PCR, and luciferase assay, data represent mean values ± SD of triplicate stimulations. Differences between groups were analyzed for statistical significance by the Student t test. Representative data from at least two independent experiments are shown in the figures.

Results

Tumor cell-conditioned medium enhances TLR ligand-induced IL-23p19 *expression in monocytes/macrophages*

To determine whether tumor-secreted factors might modulate the TLR ligand-stimulated production of IL-23 by monocytes/macrophages, we first generated medium conditioned by the lung adenocarcinoma cell line CADO-LC10. Monocytes isolated from normal human PBMC were then stimulated with PGN in the presence (LC10) or absence (medium) of the conditioned medium. PGN induced *IL-23p19* transcription in human monocytes/macrophages and the transcription was significantly increased by the presence of the conditioned medium (Fig. 1*A*, *left*). The conditioned medium alone did not induce *IL-23p19* transcription in unstimulated monocytes/macrophages (Fig. *1A*, *left*). Similar results were obtained for PBMC stimulated with BCG-CWS (Fig. 1*A*, *middle*).

We then size-fractionated the conditioned medium and the control medium into two fractions bearing the >10-kDa or <10-kDa molecules and performed the same experiment described above. The PGN-stimulated expression of *IL-23p19* in the monocytes/macrophages was more strongly enhanced by the lower molecular mass fraction (5.9-fold) than by the higher molecular mass fraction (1.7-fold) (Fig. 1*A*, *left*). Thus, it appears that the tumor cells secrete a small molecule that augments TLR ligand-induced IL-23p19 expression in monocytes/macrophages.

We also examined the effect of the conditioned medium on the transcriptional expression of *IL-12/23p40* in human PBMC. Although the unfractionated medium and the higher molecular mass

fraction clearly enhanced the transcription of *IL-12/23p40*, the lower molecular mass fraction did not (Fig. 1*A*, *right*, and data not shown). The enhancement of IL-12/23p40 expression was significantly inhibited by the anti-GM-CSF receptor α-chain Ab, suggesting that GM-CSF in the conditioned medium mainly enhanced IL-12/23p40 expression (data not shown).

The conditioned medium also enhanced the PGN-induced secretion of IL-23 by the mouse macrophage-like cell line J774.1 (Fig. 1*B*).

The conditioned medium enhances IL-23p19 *promoter activity*

To examine the effect of the conditioned medium on *IL-23p19* gene promoter activity, we performed a luciferase reporter assay using p19-5′ luc, which is a luciferase reporter plasmid containing the 6.7-kb 5′-flanking DNA region of the human *IL-23p19* gene (Fig. 1*C*). We first established several stable J774.1 cell lines that contained the reporter plasmid p19-5′ luc (J774-p19–5′ luc cells). When these cell lines were stimulated with PGN, *IL-23p19* promoter activity was increased (Fig. 1*D*, *left*). A further increase was observed when the cells were treated with PGN in the presence of the conditioned medium (Fig. 1*D*, *left*). Here again, the lower molecular mass fraction of the conditioned medium was proficient in stimulating *IL-23p19* promoter activity (Fig. 1*D*, *left*). We also generated additional luciferase reporter cells (J774-p19-5′ 2.7k luc) from p19-5′ 2.7k luc that contained only the 2.7-kb 5′-flanking region of the human *IL-23p19* gene (Fig. 1*C*). The reporter activity of this plasmid in J774.1 cells was increased by TLR stimuli (BCG-CWS and PGN) and this effect was further increased by the conditioned medium (data not shown).

Thus, the conditioned medium augments the stimulatory effect of TLR ligands on *IL-23p19* promoter activity.

Characterization of the small molecule in the conditioned medium responsible for the increase in TLR-stimulated IL-23p19 *promoter activity*

To identify the small molecule in the conditioned medium, we subjected the conditioned medium to further molecular size fractionation that separated the molecules at the nominal molecular mass of 500 Da. The <500-Da fraction, but not the >500-Da fraction, increased the *IL-23p19* promoter activity in TLR ligand-stimulated J774-p19-5′ luc (data not shown). The enhancing activity of the entire conditioned medium was not diminished by treatment with proteinase K (Fig. 1*D*, *right*) or heat treatment at 90°C for 10 min (data not shown). Thus, it appeared that the tumor-secreted small molecule we were interested in would not be a protein or peptide.

Interestingly, we found that the enhancing activity of the conditioned medium varied depending on whether the medium was obtained from tumor cell cultures in DMEM (2.4 ± 0.21), RPMI 1640 (1.6 ± 0.06), or MEM (1.0 ± 0.07). DMEM was better than RPMI 1640 and MEM had no enhancing effect at all. DMEM, RPMI 1640, and MEM contain different concentrations of glucose, namely, 4.5, 2, and 1 mg/ml, respectively. To investigate whether the glucose concentration does indeed affect the subsequent enhancing activity of the conditioned medium, we generated conditioned media from CADO-LC10 cells cultured for 3 days in DMEM supplemented with low (1 mg/ml) or high (4.5 mg/ml) concentrations of glucose. The conditioned medium prepared in high glucose DMEM enhanced the TLR ligand-stimulated *IL-23p19* promoter activity in J774-p19-5′ luc cells, unlike the conditioned medium prepared in low glucose DMEM (Fig. 1*E*). A high concentration of glucose alone had no effect (Fig. 1*E*). Glucose was metabolized to pyruvic acid, which is catalyzed by lactate dehydrogenase (LDH) to generate lactic acid. Because tumor cells show up-regulated glycolysis, even under aerobic conditions, they generally secrete large amounts of lactic acid into the culture medium (29–31). Indeed, the conditioned media of CADO-LC10

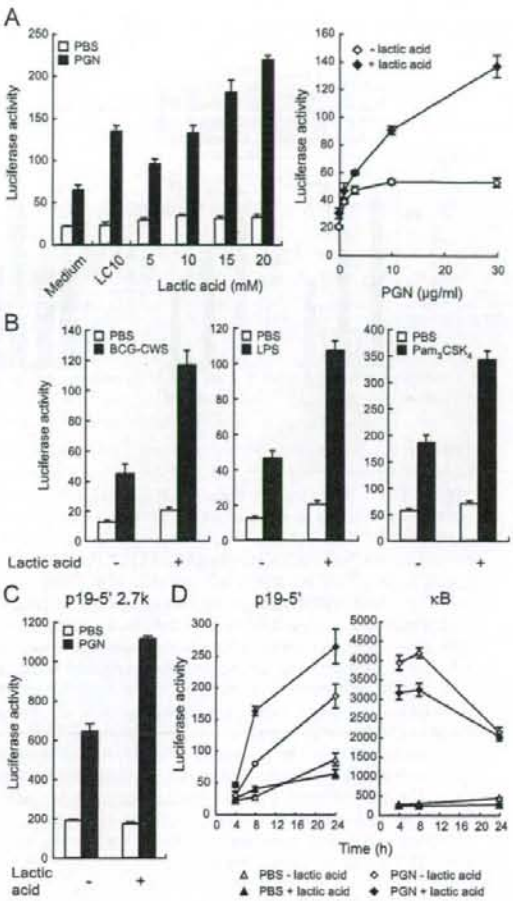

FIGURE 2. Lactic acid enhances TLR ligand-induced human *IL-23p19* promoter activity. *A*, J774-p19-5′ luc cells were stimulated with 10 μg/ml PGN in the presence of 0 (Medium), 5, 10, 15, or 20 mM lactic acid (*left*) or with 0, 2.5, 5, 10, or 30 μg/ml PGN in the presence of 15 mM lactic acid (*right*). *B*, J774-p19-5′ luc cells were stimulated with 10 μg/ml BCG-CWS (*left*), 100 ng/ml LPS (*middle*), or 100 ng/ml Pam_3CSK_4 (*right*) in the presence or absence of 15 mM lactic acid. *C*, J774-p19-5′ 2.7k luc cells were stimulated with 10 μg/ml PGN in the presence or absence of 15 mM lactic acid. *D*, J774-p19-5′ luc cells (*left*) and J774-2κB luc cells (*right*) were stimulated with 10 μg/ml PGN in the presence or absence of 15 mM lactic acid. After incubation for 4, 8, and 24 h, the cells were lysed and their luciferase activities were measured. The data represent mean values ± SD ($n = 3$).

cells cultured in 4.5 or 1 mg/ml glucose were found to contain 26.4 and 7.8 mM lactic acid, respectively (final concentrations of 13.2 and 3.9 mM in our assay). Therefore, we hypothesized that lactic acid may be the most likely candidate tumor cell-secreted factor that enhances TLR ligand-stimulated *IL-23p19* transcription.

Lactic acid in the conditioned medium enhances the IL-23p19 *gene expression induced by TLR ligands*

To examine whether lactic acid indeed enhances the *IL-23p19* gene expression induced by TLR ligands, J774-p19-5′ luc cells were stimulated with PGN in the presence of lactic acid. The luciferase activity in J774-p19-5′ luc cells was increased by lactic acid in a dose-dependent manner (Fig. 2*A*, *left*) and this enhancing

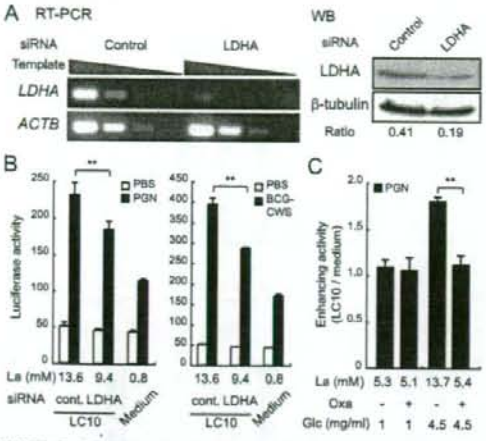

FIGURE 3. Inhibiting the production of lactic acid blocks the enhancing activity of the conditioned medium. *A*, CADO-LC10 cells were transfected with siRNA for the human *LDHA* gene (LDHA) or negative control siRNA (Control). The inhibitory effect of *LDHA* siRNA was assessed by semi-quantitative RT-PCR (*left*) and Western blotting (WB; *right*). cDNA templates prepared from siRNA-transfected CADO-LC10 cells were serially diluted (1, 0.1, 0.01, and 0.001) and amplified with *LDHA* and *β-actin* (*ACTB*) primers. Cell lysates of siRNA-transfected CADO-LC10 cells were immunoblotted with anti-LDHA or anti-β-tubulin Abs. The normalized protein expression levels of LDHA are shown below the picture. *B*, J774-p19-5′ luc cells were cultured with the conditioned media prepared from siRNA-transfected CADO-LC10 cells in the presence of 10 μg/ml PGN (*left*) or 10 μg/ml BCG-CWS (*right*) for 24 h. *C*, Alternatively, CADO-LC10 cells were incubated in low or high glucose DMEM with 20 mM oxamic acid (Oxa), an inhibitor of LDH. J774-p19-5′ luc cells were cultured with these conditioned media in the presence of 10 μg/ml PGN for 24 h. The data indicate the relative enhancing activity of CADO-LC10 conditioned medium over that of the average of control medium. The concentration of lactic acid (La) in each conditioned medium was measured in *B* and *C*. The data represent mean values ± SD ($n = 3$). **, $p < 0.01$.

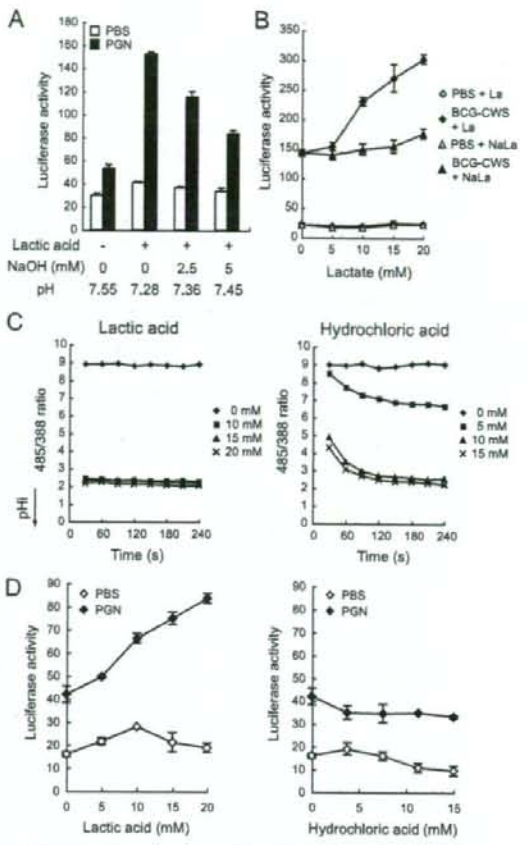

FIGURE 4. The enhancing activity of lactic acid is dependent on the pH of the medium. *A*, pH of the medium containing 15 mM lactic acid (pH 7.28) was adjusted to 7.36 and 7.45 with 2.5 and 5 mM NaOH, respectively. J774-p19-5′ luc cells were stimulated with 10 μg/ml PGN in the presence of these media. *B*, J774-p19-5′ luc cells were stimulated with 10 μg/ml BCG-CWS in the presence of 0, 5, 10, 15, or 20 mM lactic acid (La) or sodium lactate (NaLa). *C*, BCECF-loaded J774-p19-5′ luc cells were incubated with 0, 10, 15, or 20 mM lactic acid (*left*) or 0, 5, 10, or 15 mM hydrochloric acid (*right*). Intracellular pH (pHi) was detected by examining the fluorescent pH dye BCECF every 30 s as described in *Materials and Methods*. The ratio of fluorescence at 535 nm after excitation at 485 nm/388 nm was calculated. *D*, J774-p19-5′ luc cells were stimulated with 10 μg/ml PGN in the presence of various concentrations of lactic acid (*left*) or hydrochloric acid (*right*). After a 24-h incubation, the cells were lysed and the luciferase activity was measured. The data represent mean values ± SD ($n = 3$).

effect was observed at all concentrations of PGN (Fig. 2*A*, *right*). However, lactic acid alone had no detectable effect in this assay (Fig. 2*A*, *left*, □). Lactic acid at 10 mM was as effective as the conditioned medium, which contained 27.3 ± 1.09 mM lactic acid (final concentration of 13.7 ± 0.55 mM in our assay; Fig. 2*A*, *left*). The enhancing activity of lactic acid was also observed with cells stimulated with not only PGN but also other TLR ligands, namely, BCG-CWS, LPS, and Pam_3CSK_4 (Fig. 2*B*).

We next examined the region in the *IL-23p19* promoter that was responsive to lactic acid by using J774-p19-5′ 2.7k luc cells. DNA elements responsible for this enhancing activity of lactic acid like the conditioned medium were detected in a 2.7-kb 5′-flanking region of the human *IL-23p19* gene (Fig. 2*C*). Searching of a TRANSFAC database (32) with the TFSEARCH program version 1.3 (http://www.rwcp.or.jp/papia/) revealed four predicted NF-κB binding sites in a 2.7-kb 5′-flanking region (Fig. 1*B*, arrowheads). However, when we constructed J774.1 cells transfected with a luciferase reporter construct carrying canonical NF-κB binding sites and tested their responses to TLR ligands in the presence or absence of lactic acid, we did not observe any enhancing activity (Fig. 2*D*).

To test whether the lactic acid secreted from the tumor cells is indeed responsible for augmenting the TLR ligand-induced *IL-23p19* promoter activity, we inhibited the production of lactic acid from CADO-LC10 cells with *LDHA*-specific siRNA. The expression of *LDHA* mRNA (Fig. 3*A*, *left*) and protein (Fig. 3*A*, *right*) in *LDHA* siRNA-transfected cells was reduced to <10 and 50% of that of control siRNA-transfected cells, respectively. We examined enhancing activity using these conditioned media (Fig. 3*B*). Alternatively, we inhibited the LDH activity by adding oxamic acid, an inhibitor of LDH (Fig. 3*C*). Both treatments significantly reduced the concentration of lactic acid in the conditioned medium and this was matched with a decreased ability of the conditioned medium to enhance TLR ligand-stimulated *IL-23p19* promoter activity (Fig. 3, *B* and *C*). Thus, the lactic acid secreted by the tumor cells was largely responsible for the enhancing effect of the conditioned medium.

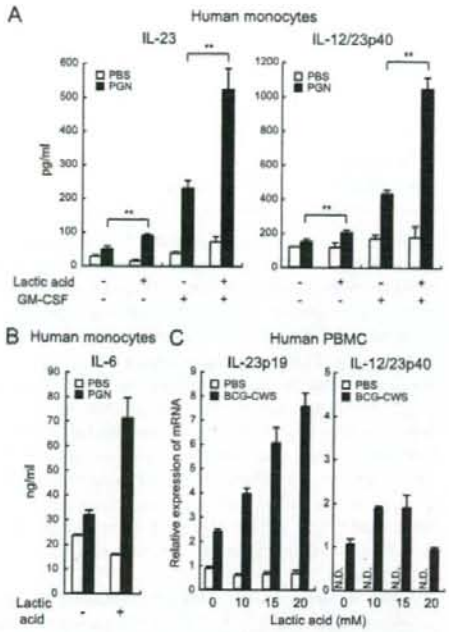

FIGURE 5. Lactic acid enhances proinflammatory cytokine production by TLR ligand-stimulated human primary monocytes/macrophages. *A*, Human monocytes were cultured for 24 h in the presence or absence of 15 mM lactic acid with or without 5 unit/ml GM-CSF. The cells were then stimulated with 10 μg/ml PGN for 24 h and the supernatants were collected. The IL-23 heterodimer and IL-12/23p40 concentrations were measured by ELISA. *B*, Human monocytes were cultured for 24 h in the presence or absence of 15 mM lactic acid. The cells were then stimulated with 10 μg/ml PGN for 24 h and the IL-6 concentrations of the supernatants were measured by ELISA. *C*, Human PBMC were stimulated with 5 μg/ml BCG-CWS in the presence of 0, 10, 15, or 20 mM lactic acid. After 4 h, *IL-23p19* (*left*) and *IL-12/23p40* (*right*) transcripts were measured by real-time RT-PCR. Relative expression of these transcripts was normalized to *β-actin* expression. N.D., Not detected. The data represent mean values ± SD ($n = 3$). **, $p < 0.01$.

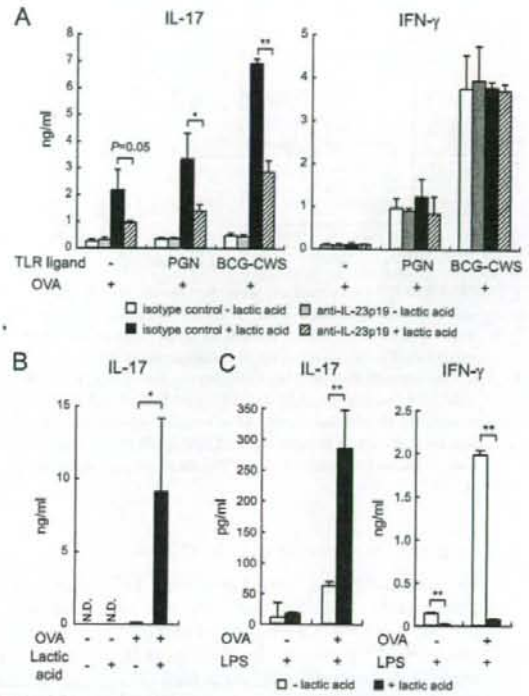

FIGURE 6. The IL-17 production by Ag-stimulated mouse splenocytes is augmented by lactic acid. *A*, Splenocytes from OT-II mice were stimulated with (■ and ▨) or without (□ and ▤) 15 mM lactic acid and PBS, 10 μg/ml PGN, or 1 μg/ml BCG-CWS. Anti-IL-23p19 Ab (▤ and ▨) or isotype control rat IgG1 (□ and ■) was also present, along with 0.2 μg/ml $OVA_{323-339}$ peptide. *B*, Splenocytes from OT-II mice were stimulated with or without 0.2 μg/ml OVA peptide and 15 mM lactic acid. *C*, Splenocytes from OT-II mice were stimulated with 100 ng/ml LPS and 0.2 μg/ml OVA peptide in the presence (■) or absence (□) of 15 mM lactic acid. The supernatants were collected after 4 days and the IL-17 and IFN-γ concentrations were measured by ELISA. N.D., Not detected. The data represent mean values ± SD ($n = 3$). *, $p < 0.05$ and **, $p < 0.01$.

Pathway involved in the enhancing activity of lactic acid

Lactate anions are transported together with protons into cells by monocarboxylate transporters (MCTs) in a pH-dependent manner (33). Therefore, to examine whether the enhancing activity of lactic acid depends on the pH of the medium, we incubated J774-p19-5' luc cells with 15 mM lactic acid in the presence of NaOH, which altered the pH of the medium (Fig. 4*A*). The enhancing activity of lactic acid was decreased in a NaOH dose-dependent manner. Furthermore, sodium lactate did not show any enhancing activity (Fig. 4*B*). The intracellular pH of the cells decreased rapidly upon incubation with lactic acid (Fig. 4*C*, *left*), suggesting that protons were transported into the cells along with lactic acid. However, in contrast to lactic acid, hydrochloric acid, which also decreased the intracellular pH, had no enhancing effect (Fig. 4, *C*, *right*, and *D*). These results suggest that only the lactate anion in its transportable state, but not the neutralized lactate anion or proton, was responsible for the enhancing activity.

Lactic acid enhances secretion of proinflammatory cytokines by human monocytes/macrophages

The IL-23p19 subunit is covalently linked to the IL-12/23p40 subunit to form an IL-23 heterodimer. The heterodimer is secreted by monocytes/macrophages/DCs stimulated with TLR ligands (5, 34). To investigate whether lactic acid enhances IL-23 secretion, human monocytes were stimulated with PGN in the presence of lactic acid for 24 h (Fig. 5*A*, *left*). The secretion of IL-23 was enhanced 1.8-fold by lactic acid. When GM-CSF was only present, IL-23 secretion was elevated 4.7-fold. When lactic acid and GM-CSF were both present, IL-23 secretion was enhanced 10.6-fold. Similarly, the PGN-induced secretion of IL-12/23p40 was slightly increased by lactic acid but synergistically enhanced by the further addition of GM-CSF (Fig. 5*A*, *right*). These results indicate that lactic acid and GM-CSF cooperate to stimulate TLR ligand-induced IL-23 and IL-12/23p40 production by human monocytes/macrophages. Furthermore, lactic acid also enhanced the secretion of another proinflammatory cytokine, IL-6, from human monocytes/macrophages stimulated with the TLR ligand (Fig. 5*B*).

We also observed that BCG-CWS increased *IL-23p19* transcription in PBMC, and like the conditioned medium (Fig. 1*A*, *middle*), lactic acid significantly enhanced this response in a dose-dependent manner (Fig. 5*C*, *left*). Conversely, lactic acid did not increase *IL-12/23p40* transcription (Fig. 5*C*, *right*), suggesting that lactic acid specifically acts on *IL-23p19* transcription.